Thermodynamic Equilibrium of Organic-Electrolyte Mixtures in Aerosol Particles

Yi Ming
Dept. of Civil and Environmental Engineering

Lynn M. Russell
Dept. of Chemical Engineering

Princeton University, Princeton, NJ 08544

This thermodynamic model describes the phase equilibria of mixtures of electrolytes and organic species in aqueous solutions existing as aerosol particles. The activity coefficient of each species in solution is explicitly related to the chemical composition by treating the (inorganic) ion−water, organic−water and ion-organic interactions with a combined Pitzer−UNIFAC thermodynamic approach. It was parameterized with a new type of multifunctional "meta-group" to better represent measured properties of long-chain monofunctional compounds and short-chain multifunctional compounds. Interactions between dissolved electrolytes and organic species are modeled using the "salting-out" effect of NaCl with organic compounds to predict the hygroscopic growth of particles composed of a salt and diacid. The predicted growth agrees well with laboratory measurements. The presence of 50% malonic acid decreases the growth of pure $(NH_4)_2SO_4$ by 20% at high relative humidities, while mixtures with 50% succinic acid and 50% glutaric acid cause decreases of 35% and 38%, respectively. The mixing of organic compounds with solubility higher than 4 $mol \cdot L^{-1}$ with salt can decrease the observed DRH. The mixture of malonic acid and $(NH_4)_2SO_4$ is predicted to start taking up water at 58%, much lower than the DRH of pure $(NH_4)_2SO_4$ (80%). Insoluble compounds do not change the observed DRH, while reducing the amount of water taken up. The predicted water contents for internal and external mixtures are largely similar, with small differences predicted for mixtures of soluble organic species. The largest deviation of 10% between the water contents of internal and external mixtures occurs for 50% malonic acid with 50% $(NH_4)_2SO_4$. For less soluble compounds such as succinic acid and glutaric acid, the two types of growth generally agree within 3%.

Introduction

Aerosol particles in the atmosphere often consist of complex mixtures of inorganic and organic compounds (Duce et al., 1983; Rogge et al., 1993; Middlebrook et al., 1998). Historically, hygroscopic properties of aerosol have been attributed to the inorganic fraction of the particles (Köhler, 1921; Meng et al., 1995). The behavior of common salts, such as NaCl and $(NH_4)_2SO_4$, and their combinations was measured precisely (Tang et al., 1986; Tang and Munkelwitz, 1994). A series of thermodynamic models have been developed that use these experimental data and specific mixing rules to predict the properties of mixtures that have not been measured (Wexler and Seinfeld, 1991; Clegg et al., 1998).

Organic compounds are emitted into the atmosphere by a variety of natural and anthropogenic sources. Organic species account for up to 50% of the total aerosol mass at marine and urban locations (Middlebrook et al., 1998; Turpin et al., 1991). The amount of water absorbed by aerosol particles at subsaturated relative humidity (RH) can be significantly altered by the presence of organics (Saxena et al., 1995; Saxena and Hildemann, 1997). In addition, there is some evidence that particles dominated by organic species are capable of acting as cloud condensation nuclei (CCN) (Cruz and Pandis,

Correspondence concerning this article should be addressed to L. M. Russell.

1997; Corrigan and Novakov, 1999; Russell et al., 2000). Despite the importance of organic compounds to the behavior of particles in the atmosphere, they have not been incorporated into computer models used to estimate phase equilibria of aerosol at different temperatures and relative humidities in the atmosphere (Wexler and Seinfeld, 1991).

Modeling of organic aerosol is handicapped by two gaps in our current knowledge. First, the chemical composition of organic particulate matter is very complex and not well understood. Typically only 10% or less of the total organic mass in particles can be identified as individual compounds by field sampling and analysis (Rogge et al., 1993). Saxena and Hildemann (1996) examined the available solubility and vapor pressure data of organic compounds and concluded that compounds with between two (C2) and seven (C7) carbon atoms and more than one functional group (multifunctional) were among the most likely water-soluble organic species in the atmosphere. Multifunctional organic compounds are also known to dominate in natural aerosol sources, such as sea salt particles (Ming and Russell, 2001). The second obstacle is the lack of thermodynamic models applicable to organic compounds of various structures and their mixtures. The available empirical models describing the organic solution are not able to represent multifunctional organic species accurately (Pividal and Sandler, 1990; Ansari and Pandis, 2000; Clegg et al., 2001). In this article, we introduce an approach to calculating the phase equilibria of complex mixtures of organic species (including multifunctional compounds) with electrolytes in particles, using a generalized semi-empirical approach modified from the work of Li et al. (1994) in a self-consistent framework for calculating activity coefficients analogous to that described by Clegg et al. (2001).

Phase Equilibrium

The Gibbs free energy (G) of a particle with coexisting liquid and solid phases suspended in a vapor is expressed as

$$G = \mu_S n_S + \mu_L n_L + \mu_V n_V + \sigma^{LV} a^{LV} + \sigma^{SL} a^{SL} \quad (1)$$

where the subscripts S, L, and V refer to the solid, liquid, and vapor phases (assuming only one phase of each type), respectively. μ is the chemical potential, and n is the number of moles of each phase. σ^{LV} and σ^{SL} are the interfacial tensions on the surface areas a^{LV} between liquid and vapor phases and a^{SL} between solid and liquid phases (Mirabel et al., 2000).

The phase equilibrium system of aerosol is composed of one vapor phase V, liquid phases with index l, and solid phases with index s coexisting. Based on Eq. 1, the total Gibbs free energy of the system (G) for a particle with multiple ionic species i, organic species o, and water partitioned into one or more liquid phases l or solid phases s is

$$G = \sum_s \left(\sum_i n_i^s \mu_i^s + \sum_o n_o^s \mu_o^s \right) + \sum_l \left(\sum_i n_i^l \mu_i^l + \sum_o n_o^l \mu_o^l + n_w^l \mu_w^l \right) + n_w^V \mu_w^V + \sum_l \sigma^{lV} a^{lV} + \sum_l \sum_s \sigma^{sl} a^{sl} \quad (2)$$

The contributions to the total Gibbs free energy are from both the chemical potential of species present in all phases and from the interfacial energy caused by the interfacial tension σ over the interfacial area a between these phases.

Before mixing, the initial state for water is vapor as quantified by relative humidity RH, whereas the initial states for organic and ionic species are their respective pure solids. Thus, the total initial Gibbs free energy G^o that describes each of the species in its unmixed state is expressed as

$$G^o = \sum_s \left(\sum_i n_i^s \mu_i + \sum_o n_o^s \mu_o \right) + \sum_l \left(\sum_i n_i^l \mu_i + \sum_o n_o^l \mu_o + n_w^l \mu_w^V \right) + n_w^V \mu_w^V \quad (3)$$

where μ_o and μ_i are the chemical potentials of organic and inorganic species at their respective pure solid states.

Noting that

$$\mu_o = \mu_o^s \quad (4)$$

$$\mu_i = \mu_i^s \quad (5)$$

if the unmixed solid states are pure solid phases, the change in Gibbs free energy due to mixing ΔG is given by

$$\Delta G \equiv G - G^o = \sum_l \left[\sum_i \left(\mu_i^l - \mu_i \right) n_i^l + \sum_o \left(\mu_o^l - \mu_o \right) n_o^l + \left(\mu_w^l - \mu_w^V \right) n_w^l \right] + \sum_l \sigma^{lV} a^{lV} + \sum_l \sum_s \sigma^{sl} a^{sl} \quad (6)$$

The chemical potentials can be written in terms of their reference state chemical potentials (μ_i^o, μ_o^o, μ_w^o) and their activities as follows:

(i) inorganic ions:

$$\mu_i^l = \mu_i^o + RT \ln \left(x_i^l \gamma_i^l \right) \quad (7)$$

$$\mu_i^s = \mu_i^o + RT \ln \left(\bar{x}_i^l \bar{\gamma}_i^l \right) \quad (8)$$

(ii) organic species:

$$\mu_o^l = \mu_o^o + RT \ln \left(x_o^l \gamma_o^l \right) \quad (9)$$

$$\mu_o^s = \mu_o^o + RT \ln \left(\bar{x}_o^l \bar{\gamma}_o^l \right) \quad (10)$$

(iii) water:

$$\mu_w^l = \mu_w^o + RT \ln \left(x_w^l \gamma_w^l \right) \quad (11)$$

$$\mu_w^V = \mu_w^o + RT \ln \left(\frac{RH}{100} \right) \quad (12)$$

where x and γ are the mole fraction and activity coefficient, respectively. $\bar{x}$ and $\bar{\gamma}$ refer to the mole fraction and activity coefficient at the solubility limit of the pure solid. By substituting Eqs. 7–12 into Eq. 6, the chemical potentials at their

respective reference states are cancelled so that the Gibbs free energy change ΔG simplifies to

$$\Delta G \equiv G - G^o = RT \sum_l \sum_i \ln\left(\frac{x_i^l \gamma_i^l}{\bar{x}_i^l \bar{\gamma}_i^l}\right) n_i^l + RT \sum_l \sum_o \ln\left(\frac{x_o^l \gamma_o^l}{\bar{x}_o^l \bar{\gamma}_o^l}\right) n_o^l + RT \sum_l \ln\left(\frac{\frac{x_w^l \gamma_w^l}{RH}}{100}\right) n_w^l + \sum_l \sigma^{lV} a^{lV} + \sum_l \sum_s \sigma^{sl} a^{sl} \quad (13)$$

The distribution of species among phases at chemical equilibrium is determined by minimizing the Gibbs free energy change ΔG. In our work, the total amount of each nonwater component in the equilibrium system is fixed in order to compare results with a constant dry mass basis. At specific relative humidity, the amount of water in the liquid phases is allowed to vary to achieve the configuration of lowest Gibbs free energy. In searching for the optimal water content, the number of solution phases and the amounts of each component in each phase are also allowed to vary to find the lowest Gibbs free energy change. The compounds with similar polarities have a tendency to form a homogeneous solution, while different polarities cause species to separate from each other due to the nonideality of resulting solutions (Saxena and Hildemann, 1996).

Noting that

$$\bar{x}_k^l \bar{\gamma}_k^l = \frac{f_k^l}{f_k^s} \quad (14)$$

where f_k^l is the pure liquid fugacity and f_k^s is the pure solid fugacity, and that the equilibrium constant at solubility limit K_i^{eq} can be rewritten as $\bar{x}_k^l \bar{\gamma}_k^l = K_i^{eq}$ for electrolytes, we can rewrite Eq. 13 as

$$\Delta G \equiv G - G^o = RT \sum_l \sum_i \ln\left(\frac{x_i^l \gamma_i^l}{K_i^{eq}}\right) n_w^l + RT \sum_l \sum_o \ln\left(\frac{\frac{x_o^l \gamma_o^l}{f_o^l}}{f_o^S}\right) n_o^l + RT \sum_l \ln\left(\frac{\frac{x_w^l \gamma_w^l}{RH}}{100}\right) n_w^l + \sum_l \sigma^{lV} a^{lV} + \sum_l \sum_s \sigma^{sl} a^{sl} \quad (15)$$

The values of K_i^{eq} for various salts are compiled in Clegg et al. (1998). The approach to calculating the fugacity ratio of organic compounds is based on an empirical model of organic properties described in the next section.

The activity coefficient γ_i^l of component i in solution l is a function of the chemical composition represented by x_n^l, $n = 1, 2, \ldots, N$ (N is the number of species present). In order to evaluate the Gibbs free energy change ΔG as shown by Eq. 15, we need to describe the activity coefficients as functions of the composition. This model of solution activity, coupled with a composition-dependent parameterization of surface tension, allows us to search for the minimum Gibbs free energy at a specified composition and thus to identify the equilibrium phase partitioning of the system.

Solution Activity

While cloud droplets are frequently sufficiently dilute to allow us to assume that solute activities are linearly dependent on mole fractions, subsaturated particles at relative humidities between 35% and 95% frequently behave nonideally. In such nonideal solutions the chemical potentials of components vary both with their own mole fraction and with the overall composition. In general, two types of both electrolyte and organic solution models have been developed for a variety of applications.

Zhang et al. (2000) summarized existing models of aqueous solutions of electrolytes including the Zdanovski-Stokes-Robinson (ZSR) and Pitzer approaches. One such model is the Pitzer-Simonson-Clegg model, based on the concept of ion interaction in which interactions between ions are used to describe the solution nonideality (Clegg et al., 1992).

Unlike electrolytes, organic species have diverse chemical structures and possess quite different properties, both from each other and from electrolytes. The concept of group contribution methods (GCM) utilizes functional groups, instead of molecules, as the interacting entities in order to reduce to about 20 groups the number of parameters needed to describe hundreds of organic species (Fredenslund et al., 1977). UNIFAC (UNIQUAC Functional Group Activity Coefficients Model, where UNIQUAC stands for Universal Quasi-Chemical) uses a GCM-based approach and has been shown to be effective in predicting the properties of mixtures in various applications (Gmehling, 1995). The phase equilibrium model for internal mixtures of organics and electrolytes that we have developed is based on the Pitzer-Simonson-Clegg approach to electrolytes and the UNIFAC approach to organic species. Since pure organic and pure electrolyte solutions are limiting cases of the general model, the accuracy of mixture predictions is expected to be comparable to existing models (Clegg et al., 2001).

Three different types of components are presented in the solution. They are inorganic ions (electrolytes), organic compounds, and water. The activity coefficient of each component varies with particle composition, namely the mole fraction x_m of a species m, where

$$x_m = \frac{n_m}{n_w + \sum_o n_o + \sum_i n_i} \quad (16)$$

The subscripts w, o, and i of mole number n represent water, organic compound, and ion, respectively. The summations are over all organic compounds and ions present in the system. The binary interactions involved in the general model are ion-water (IW) and organic-water/organic-ion (OW/OI), where here we use "ion" to refer only to inorganic ions (Kikic et al., 1991). The activity coefficient of each component γ_m includes contributions from these two types of interactions, as described by

$$\ln \gamma_m = \ln \gamma_m^{IW} + \ln \gamma_m^{OW/OI} \quad (17)$$

where independent interactions are assumed to have additive contributions (Li et al., 1994). The ion-water interactions are calculated as in previously proposed models (Clegg et al., 1992; Wexler and Seinfeld, 1991). Organic-water and organic-ion interactions are described with a UNIFAC-based approach using measurements of "salting-out" constants for different ions (Kikic et al., 1991; Yan et al., 1999; Sutton and Calder, 1974). Recent work has also calculated properties for specific binary (single inorganic ion-single organic species-water) mixtures for which detailed data are available (Clegg et al., 2001). In this work, we use a general approach to quantify electrolyte-organic interactions in aqueous solutions that accurately represents the range of species commonly found in atmospheric particles. The following sections describe the algorithms that underly these three different types of molecular interactions in order to calculate the phase equilibrium.

Ion-water interactions

The Pitzer-Simonson-Clegg model is used to calculate the ion-water contribution γ_m^{IW} in Eq. 17 to the overall activity coefficient γ_m (Clegg et al., 1992). The interactions between ions and water molecules are considered to be independent of the organic species existing in solution (all corrections for interactions with organic species are included in $\gamma_m^{OW/OI}$). The inorganic mole fraction $x_m^{\star}$ appropriate in this context is the number of moles of ions normalized by the total number of non-organic constituents, namely

$$x_m^{\star} = \frac{n_m}{n_w + \sum_i n_i} \tag{18}$$

where m refers to either a water molecule or an ion (Clegg et al., 2001). The electrolyte-water contribution to activity coefficient γ_m^{IW} is the combination of long-range (LR) and short-range (SR) effects

$$\ln \gamma_m^{IW} = \ln \gamma_m^{LR} + \ln \gamma_m^{SR} \tag{19}$$

where the specific expressions for γ_m^{LR} and γ_m^{SR} are given by Eq. 24–26 and Eq. 15–17 of Clegg et al. (1992). Short-range interactions dominate in concentrated solutions and long-range in dilute solutions.

A complete parameter set for experimental data for Na^+, NH_4^+, H^+, Cl^-, SO_4^{2-} and HSO_4^- is available from Clegg et al. (1998). Two additional ions of interest in marine air (Mg^{2+} and Ca^{2+}) have been added using parameters in Clegg et al. (1992). The missing binary and ternary interaction parameters were set to zero. The model predictions agreed with existing mixture data for systems composed of Na^+—Mg^{2+}—Cl^-—H_2O, Na^+—Mg^{2+}—SO_4^{2-}—H_2O, Na^+—Cl^-—SO_4^{2-}—H_2O, and Ca^{2+}—Mg^{2+}—Cl^-—H_2O within 1% (Clegg et al., 1992). Since Mg^{2+} and Ca^{2+} account for small fractions of inorganic mass in seawater (Mg^{2+} 3.7%, Ca^{2+} 1.1%) (Riley and Chester, 1971), the error introduced by setting missing parameters to zero is negligible for sea salt aerosol. For other types of aerosol, in which Mg^{2+} and Ca^{2+} and other ions that we have omitted (such as NO_3^-) are more prevalent, more detailed laboratory results on the interactions of these ions are needed. The accuracy of the inorganic ion interactions with water is illustrated in Figure 1.

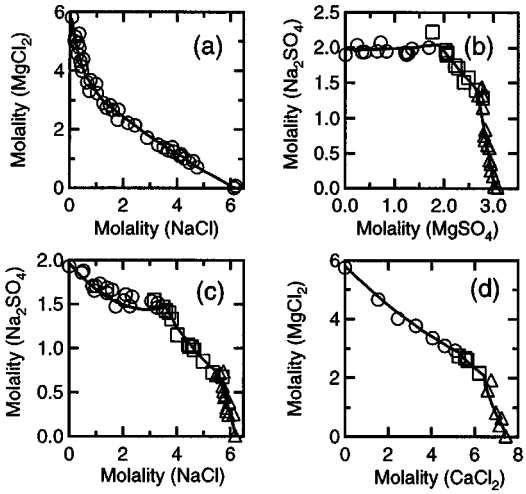

Figure 1. Correlated solubilities of salts in four ternary ion solutions with measurements.

(a): NaCl (open circle) in Na-Mg-Cl-H_2O solution; (b): $Na_2SO_4{\cdot}10H_2O$ (open circle), $Na_2Mg(SO_4)_2{\cdot}4H_2O$ (open square), and $MgSO_4$ (open triangle) in Na-Mg-SO_4-H_2O solution; (c): $Na_2{\cdot}10H_2O$ (open circle), Na_2SO_4 (open square), and NaCl (open triangle) in Na-Cl-SO_4-H_2O solution; (d): $MgCl_2{\cdot}6H_2O$ (open circle), $Mg_2CaCl_6{\cdot}12H_2O$ (open square), and $CaCl_2{\cdot}6H_2O$ (open triangle) in Mg-Ca-Cl-H_2O solution. Experimental data are compiled in Silcock (1979).

The activity coefficients $\gamma_m^{LR\star}$ and $\gamma_m^{SR\star}$ are translated from the inorganic-only mole fraction ($x_m^{\star}$) to the solution mole fraction (x_m) in order to obtain γ_m^{LR} and γ_m^{SR} using the following relationship

$$\ln \gamma_m^{LR} = \ln \gamma_m^{LR\star} - \ln\left(1 - \sum_o x_o\right) \tag{20}$$

$$\ln \gamma_m^{SR} = \ln \gamma_m^{SR\star} - \ln\left(1 - \sum_o x_o\right) \tag{21}$$

These activity coefficients can then be used to calculate γ_m^{IW} with Eq. 19.

Organic-water and organic-ion interactions

In the original UNIFAC model (Fredenslund et al., 1975), the contribution to the activity coefficient of each component m in solution comes from two sources: the combinatorial part (γ_m^C) and the residual part (γ_m^R)

$$\ln \gamma_m^{OW/OI} = \ln \gamma_m^C + \ln \gamma_m^R \tag{22}$$

Here m refers to organic compounds, inorganic compounds, or water. The expressions for $\ln \gamma_m^C$ and $\ln \gamma_m^R$ were given by Eq. 2 to Eq. 9 of Fredenslund et al. (1975).

Limitations of UNIFAC models preclude their use for predicting aerosol properties (Saxena and Hildemann, 1997; Ansari and Pandis, 2000). The original purpose of UNIFAC was to assist the design of chemical separation processes (Gmehling, 1995). For these applications, the compounds of

most interest are small monofunctional compounds with solution systems that are usually highly concentrated. However, common organic species in atmospheric particles include both long-chain monofunctional and short-chain multifunctional compounds (Saxena and Hildemann, 1997). Water can account for a large fraction of aerosol mass, making the solution both dilute and polar. This mismatch of mixture type in traditional UNIFAC models means that existing correlation parameters will not accurately describe aerosol phase equilibrium for the complex solutions found in the atmosphere. In addition to correlating data with appropriate measurement data sets, the model accuracy can be improved by defining more specific types of functional groups that use different compounds for correlation.

The proximity of two or more polar functional groups in the same multifunctional compounds make the assumption of independent groups inappropriate (Pividal and Sandler, 1990). Wu and Sandler (1989, 1991) provided proof for the strong interaction between polar groups within a molecule from *ab initio* molecular orbital calculations. To improve the prediction of the behavior of multifunctional organics, new "meta-groups" for different combinations of groups were correlated from available experimental data (Wu and Sandler, 1991). For example, to account for the effects of multiple functional groups in one molecule, we define meta-groups consisting of pairs of functional groups, as shown in Table 1 (for example, —COOH in hydroxy-acids, —OH in monosaccharides, and —COOH in diacids). In addition, multiple types of alkyl groups, CH_n ($n = 0,1,2,3$) can be used to represent the carbons in short-chain and long-chain alkanes, as well as in monosaccharides, hydroxy-acids and diacids. This expanded set of groups and their correlated interaction parameters are listed in Table 1.

For monofunctional compounds, most existing UNIFAC parameter sets are correlated from short-chain species with carbon numbers less than 5. These parameters cannot be used successfully to represent the infinite dilution activity coefficients (IDAC) of long-chain insoluble compounds (Zhang et al., 1998). Most nonpolar organic species measured in marine and polluted aerosol are long-chain alkanes, alkanols and carboxylic acids (Gagosian et al., 1981; Gogou et al., 1998). Zhang et al. (1998) showed that existing UNIFAC models predict infinite dilution activity coefficients of long-chain monofunctional compounds with mean relative deviations from measured values of 45% to 72%.

Dissolved electrolytes can interact with organic components in solution. The solubilities of most organic compounds are lowered with increasing salt concentrations (known as the "salting-out effect"), although some species become more soluble due to the presence of salts (known as the "salting-in" effect) (Long and McDevit, 1952). Despite the relatively small number of electrolytes, the variety of organic species and their different properties make the electrolyte-organic interaction quite complicated. We can consider this type of interaction by treating ions as groups in UNIFAC. Since the interaction between ions and water is assessed by γ_m^{IW} from the Pitzer-Simonson-Clegg model, no additional interactions for water and ions are included here. Therefore, the activity coefficients of water and ions predicted by this extended UNIFAC approach should reduce to unity for aqueous solutions of pure

Table 1. Group Interaction Parameters Used in This Model

	$Na^{+\bigstar}$	$NH^{+\bigstar}$	Cl^-	$SO_4^{2-\bigstar\bigstar}$	$-CH_n$ †	$-OH$ ††	$-COOH$ ‡	$-CH_nCO$ ‡‡
Na^+	0	0	0	0	7,794*	6,654*	6,654*	6,654*
$NH_4^{+\bigstar}$	0	0	0	0	7,794*	6,654*	6,654*	6,654*
Cl^-	0	0	0	0	8,093*	53,760*	53,760*	53,760*
$SO_4^{2-\bigstar\bigstar}$	0	0	0	0	8,093*	53,760*	53,760*	53,760*
$—CH_n$ †	7,771*	7,771*	8,107*	8,107*	0	986.5	663.5	476.4
$-OH$ ††	5,768*	5,768*	7,032*	7,032*	156.4	0	199	84
—COOH ‡	5,768*	5,768*	7,032*	7,032*	315.3	−151	0	−297.8
$—CH_nCO$ ‡‡	5,768*	5,768*	7,032*	7,032*	26.76	164.5	669.4	0
$—CH_n$ §	636*	636*	1,027*	1,027*	0	986.5	663.5	476.4
$—CH_nO$ §§	−640*	−640*	−720*	−720*	83.36	237.7	664.6	52.38
—OH ‖	184*	184*	488*	488*	156.4	0	199	84
$—CH_n$ ‖‖	1,008*	1,008*	1,491*	1,491*	0	986.5	663.5	476.4
—COOH #	−23.3*	−23.3*	−123.1*	−123.1*	315.3	−151	0	−297.8
—OH ##	208.8*	208.8*	781.6*	781.6*	156.4	0	199	84
—CH ***	1,231*	1,231*	1,593*	1,593*	0	986.5	663.5	476.4
—COOH †††	−324*	−324*	2,134*	2,134*	315.3	−151	0	−297.8
H_2O	0	0	0	0	541.3*	−959*	−530*	−471*

Parameters marked with an asterisk were correlated in this work; all other parameters were correlated by Gmehling et al. (1982).
★Experimental data were not available; parameters of Na^+ have been substituted.
★★Experimental data were not available; parameters of Cl^- have been substituted.
† —CH_n ($n = 0,1,2,3$) in long-chain monofunctional compounds.
††—OH in long-chain monofunctional compounds.
‡ —COOH in long-chain monofunctional compounds.
‡‡—CH_nCO ($n = 2,3$) in long-chain monofunctional compounds.
§ —CH_n ($n = 0,1,2,3$) in monosaccharides.
§§—CH_nO ($n = 0,1,2$) in monosaccharides.
‖ —OH in monosaccharides.
‖‖—CH_n ($n = 0,1,2,3$) in hydroxy-acids.
—COOH in hydroxy-acids.
##—OH in hydroxy-acids.
***—CH_n ($n = 0,1,2,3$) in diacids.
†††—COOH in diacids.

Table 1. Group Interaction Parameters Used in This Model (continued)

	$-CH_n^{\S}$	$-CH_nO^{\S\S}$	$-OH^{\|}$	$-CH_n^{\|\|}$	$-COOH^{\#}$	$-OH^{\#\#}$	$-CH_n^{***}$	$-COOH^{\dagger\dagger\dagger}$	H_2O
Na^+	376*	203*	147*	2,292*	1,958*	1,849*	2,532*	132*	0
NH_4^+ ★	376*	203*	147*	2,292*	1,958*	1,849*	2,532*	132*	0
Cl^-	719*	638*	366*	2,623*	2,289*	2,180*	2,864*	132*	0
SO_4^{2-} ★★	719*	638*	366*	2,623*	2,289*	2,180*	2,864*	132*	0
$—CH_n^{\dagger}$	0	251.5	986.5	0	663.5	986.5	0	663.5	1,318*
$—OH^{\dagger\dagger}$	156.4	28.06	0	156.4	199	0	156.4	199	1,000*
$—COOH^{\ddagger}$	315.3	−338.5	−151	315.3	0	−151	315.3	0	1,000*
$—CH_nCO^{\ddagger\ddagger}$	26.76	5.202	164.5	26.76	669.4	164.5	26.76	669.4	1,000*
$—CH_n^{\S}$	0	251.5	986.5	0	663.5	986.5	0	663.5	1,318*
$—CH_nO^{\S\S}$	83.36	0	237.7	83.36	664.6	237.7	83.36	664.6	2,007*
$—OH^{\|}$	156.4	28.06	0	156.4	199	0	156.4	199	−189.7*
$—CH_n^{\|\|}$	0	251.5	986.5	0	663.5	986.5	0	663.5	1318
$—COOH^{\#}$	315.3	−338.5	−151	315.3	0	−151	315.3	0	−163.3*
$—OH^{\#\#}$	156.4	28.06	0	156.4	199	0	156.4	199	−92.3*
$—CH^{***}$	0	251.5	986.5	0	663.5	986.5	0	663.5	4,694*
$—COOH^{\dagger\dagger\dagger}$	315.3	−338.5	−151	315.3	0	−151	315.3	0	−186.3*
H_2O	300	193.1*	171.3*	300	64.6*	224.4*	304*	86*	0

Parameters marked with an asterisk were correlated in this work; all other parameters were correlated by Gmehling et al. (1982).
★Experimental data were not available; parameters of Na^+ have been substituted.
★★Experimental data were not available; parameters of Cl^- have been substituted.
† —CH_n (n = 0,1,2,3) in long-chain monofunctional compounds.
†† —OH in long-chain monofunctional compounds.
‡ —COOH in long-chain monofunctional compounds.
‡‡ —CH_nCO (n = 2,3) in long-chain monofunctional compounds.
§ —CH_n (n = 0,1,2,3) in monosaccharides.
§§ —CH_nO (n = 0,1,2) in monosaccharides.
‖ —OH in monosaccharides.
‖‖ —CH_n (n = 0,1,2,3) in hydroxy-acids.
—COOH in hydroxy-acids.
—OH in hydroxy-acids.
*** —CH_n (n = 0,1,2,3) in diacids.
††† —COOH in diacids.

electrolytes. This constraint requires setting the interaction parameters describing ionic groups and water ($\alpha_{i,w}$ and $\alpha_{w,i}$ in Eq. 9 of Fredenslund et al., 1975) to zero as indicated in Table 1. The volume and area parameters R_i and Q_i of ionic group i in Eq. 4 of Fredenslund et al. (1975) are arbitrarily set equal to those for water so that the combinatorial part of the UNIFAC equations will be zero in the absence of organics. This assumption is tested in the discussion on model sensitivity.

Surface Tension Algorithm

Since the contribution of interfacial energy to the total Gibbs free energy of the multiphase equilibrium in Eq. 1 is always positive, it increases the Gibbs free energy relative to the bulk case without interfacial tension. As a result, higher relative humidities are required for smaller particles to reach equilibrium with a specified solution.

The surface tension of the solution is determined by its chemical composition. Organic species lower the surface tension of aqueous solutions to below that of pure water (Li et al., 1999). Aqueous solutions of electrolytes have higher surface tensions that pure water (Nath, 1999). In this work, both types of solutes coexist in the solution and affect the surface tension. To calculate the surface tension from the chemical composition of an electrolyte-organic aqueous solution, the solution phase is divided into a surface phase and a bulk phase. The surface phase is a thin layer immediately adjacent to the vapor phase and serves as a boundary to separate the bulk solution phase from the vapor phase. All species present in the solution are distributed between the surface and bulk phases, and the composition of the bulk phase is the same as the overall chemical composition of solution, since the mass of the surface phase is negligibly small.

The chemical composition of the surface phase is independent of the overall composition and can be determined from measured mixture properties. The chemical potential μ_m^B of component m (which may be either water or an organic species) in the bulk phase (B) is represented as

$$\mu_m^B = \mu_m^{B,o} + RT \ln\left(x_m^B \gamma_m^B\right) \tag{23}$$

where $\mu_m^{B,o}$ is the chemical potential at the reference state of m in the bulk phase. x_m^B and γ_m^B are the mole fraction and activity coefficient of m in the bulk phase. The chemical potential μ_m^S of component m in the surface layer is given by

$$\mu_m^S = \mu_m^{S,o} + RT \ln\left(x_m^S \gamma_m^S\right) - \bar{A}_m \sigma \tag{24}$$

where $\mu_m^{S,o}$ is the chemical potential at the reference state of m in the surface phase. x_m^S and γ_m^S are the mole fraction and activity coefficient of m in the surface phase. $\bar{A}_m$ is the partial molar area of m in solution and σ is the surface tension of solution. The reference states of organic components and water are their respective pure liquid phases. The chemical potentials at the reference states in the bulk and surface phase are related by

$$\mu_m^{B,o} + A_m \sigma_m = \mu_m^{S,o} \tag{25}$$

where σ_m is the surface tension of m in pure liquid phase and A_m is the corresponding molar area.

In order to reach equilibrium between the surface and bulk phases, the chemical potentials of each species in the bulk and surface phases should be equal to each other, namely

$$\mu_m^B = \mu_m^S \tag{26}$$

Substituting Eqs. 23, 24, and 25 in 26 and noting that the partial molar area $\bar{A}_m$ can be approximated as the molar area A_m (Li et al., 1999), we find

$$\sigma = \sigma_m + \frac{RT}{A_m} \ln \frac{x_m^S \gamma_m^S}{x_m^B \gamma_m^B} \tag{27}$$

For electrolytes, the concentrations of ions in the surface phase are assumed to be proportional to those in the bulk phase

$$x_{i,S} = k_i x_{i,B} \tag{28}$$

where k_i is correlated from the measurements of surface tension for each species (Li et al., 1999). Laaksonen (1993) calculated the interior concentration of aerosol particles created by dispersion of surfactant solutions depending on the overall concentration (the concentration of bulk solution from which aerosol is generated) and particle size by solving the Gibbs-Duhem equation. To assess the impact of our assumption of constant concentration, we allow the concentration to vary in the particle for two cases, $(NH_4)_2SO_4$ and glutaric acid solutions. For a 100 nm dry particle of $(NH_4)_2SO_4$, the solute increases the surface tension of the solution, the gradient in concentration between the interior and overall compositions increases the growth by 2%. Since glutaric acid lowers the surface tension of the solution, the hygroscopic growth decreases by 3%.

Empirical Correlations

Thermodynamic data collected from published measurements were used to fit the interaction parameters described above. The different types of data are summarized below:

Infinite dilution activity coefficient. The infinite dilution activity coefficient (IDAC) is the limit of the activity coefficient of a solute in water when the concentration of the solute is infinitely small. In this situation, a single solute molecule is completely surrounded by water molecules. Therefore, the IDAC largely reflects the interaction between solute and water in the absence of other solutes. Kojima et al. (1997) described an accurate method for measuring IDAC and collected a comprehensive database of available measurements for a variety of compounds. Comparisons to these data are shown in Figure 2.

Solubility and activity coefficient at saturation. At the solubility limit, the solute reaches chemical equilibrium with its pure state. For organic compound o existing as solid in the pure state, the activity at saturation is equal to the corresponding ratio of liquid-solid reference fugacities f_o^l/f_o^s

$$x_o^{\text{sat}} \gamma_o^{\text{sat}} = \frac{f_o^l}{f_o^s} \tag{29}$$

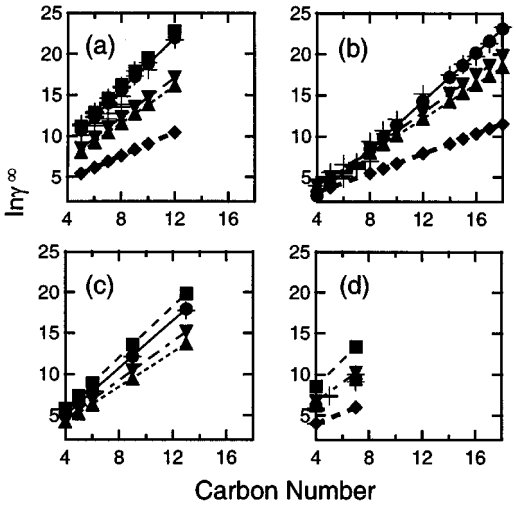

Figure 2. Correlated infinite dilution activity coefficients (γ^∞) with measurements of four types of long-chain monofunctional compounds.

(a) Alkane, (b) alcohol, (c) acid and (d) ketone. The measurements (crosses) are compiled in Kojima et al. (1997). Correlations are from this work (circles on solid line) along with predictions from the original UNIFAC (Fredenslund et al., 1977; squares on thin dashed line), VLE-UNIFAC (Skjold-Jørgensen et al., 1979; upward-pointing triangles on thin dotted line), LLE-UNIFAC (Magnussen et al., 1981; downward-pointing triangles on thin dashed-dotted line) and IDAC-UNIFAC (Bastos et al., 1988; diamonds on dashed line).

The mole fraction at the solubility limit and the activity coefficient at saturation are denoted by x_o^{sat} and γ_o^{sat}, respectively. The fugacity ratio is a quantitative measurement of energy used to melt organic solid o (Peers et al., 2000). From the enthalpy of melting ΔH_m and melting temperature T_m, the fugacity ratio at temperature T can be calculated as

$$\ln \frac{f_o^L}{f_o^S} = \frac{\Delta H_m}{RT_m}\left(\frac{T_m}{T} - 1\right) \tag{30}$$

where R is the universal gas constant. If the fugacity ratio of an organic compound is known, the activity coefficient at saturation can be calculated from the measured solubility according to Eq. 29.

Salting-out constant. The impact of dissolved electrolytes on the solubility of organic compounds was described by the Setchenow equation as

$$\log\left(\frac{C_o}{C_{o,s}}\right) = k_s C_s \tag{31}$$

where C_o and $C_{o,s}$ are the solubility of organic compound o ($\text{mol}\cdot\text{L}^{-1}$) in pure water and in aqueous salt solution, respectively. C_s is the corresponding salt concentration ($\text{mol}\cdot\text{L}^{-1}$) (Sutton and Calder, 1974). The empirical "salting-out" constant k_s is correlated from experimental data (Long and McDevit, 1952). Equation 31 assumes the organic concentration is low, in which case it can be rewritten in terms of mole fractions of organic compounds in water (x_o) and of organic

compounds in salt solution ($x_{o,s}$)

$$\log\left(\frac{x_o}{x_{o,s}}\right) = \log\left(\frac{\gamma_{o,s}}{\gamma_o}\right) = k_s C_s \tag{32}$$

where γ_o and $\gamma_{o,s}$ are the activity coefficient at saturation in pure water and in aqueous salt solution, respectively. At high organic concentrations, Eq. 31 is inaccurate. The ion-organic interaction parameters derived from these parameters are summarized in Table 1.

Using these types of thermodynamic data, the least-squares approach was used to estimate the model parameters from experimental data. The objective function

$$F(\tau) = \min \sum_j \sum_k \left(X_{j(k)} - \widehat{X}_{j(k)}\right)^2 \tag{33}$$

for any data type j, for example, β_{io} is used to minimize the difference between the measured data $X_{j(k)}$ and the fitted parameterization $\widehat{X}_{j(k)}$ for the kth measured and calculated data points, respectively. τ is the optimal parameter vector (Magnussen et al., 1981). The software package MINPACK that implements the Levenberg-Marquardt algorithm was employed to minimize the objective function and fit the model parameters (More et al., 1980). The resulting parameter set is included in Table 1. The available experimental data of aqueous solutions of organic species were used to correlate the interaction parameters between organic groups and water, and between organic and ionic groups from measurements using the datasets summarized in Table 2. For each type of correlation, Table 2 lists the data set used, the parameters derived, and the precision of the fit to the data. The following sections describe each of these fits and illustrate them graphically.

Long-chain monofunctional compounds

Most well developed UNIFAC models were based on experimental data of short-chain (less than 5 carbons) monofunctional compounds (Fredenslund et al., 1977; Skjold-Jørgensen et al., 1979; Magnussen et al., 1981). Zhang et al. (1998) reported that the available UNIFAC parameter sets cannot be reliably utilized to predict the infinite dilution activity coefficients of long-chain monofunctional compounds. The new groups listed in Table 1 are used to represent methyl (CH_n), hydroxyl (—OH), carboxylic acid (—COOH), and carbonyl (—CH_nCO—) in long-chain monofunctional compounds. The model correlations together with those from other UNIFAC models are compared with measured infinite

Table 2. Experimental Data used in Fitting Model Parameters*

Solution System	Data Type	Concentration Range	Reference	Percentage Error	UNIFAC Parameters Correlated
Alkane (C5-C12)-water Alcohol (C4-C18)-water Acid (C4-C13)-water Ketone (C4-C7)-water	Activity coefficients of organic compounds	Infinite dilution	Kojima et al. (1997)	8%	Between long-chain monofunctional organic compounds (—CH_n, —OH, —COOH, and —CH_nCO—) and water
Alkane (C12, C14, C16, C18) − NaCl-water	Activity coefficients of alkane	NaCl (0–5.3 mol L^{-1})	Sutton and Calder (1974)	7%	Between —CH_n in long-chain monofunctional compounds and ionic groups (Na^+ and Cl^-)
Hexanol-NaCl-water	Activity coefficients at solubility of hexanol	NaCl (0–5.3 mol L^{-1})	Zdenek et al. (1980)	3%	Between —OH in long-chain monofunctional compounds and ionic groups (Na^+ and Cl^-)
Glucose-water Fructose-water	Relative humidity	Glucose (0–4 mol L^{-1}) Fructose (0–6.3 mol L^{-1})	Peres and Macedo (1997)	3%	Between groups in monosaccharides (—CH_n, —CH_nO, and —OH) and water
Glucose-NaCl-water Fructose-NaCl-water	Relative humidity	Glucose, Fructose (0–3.0 mol L^{-1}) NaCl (0–3.5 mol L^{-1})	Comesana et al. (1999)	0.1%	Between groups in monosaccharides (—CH_n, —CH_nO and —OH) and ionic groups (Na^+ and Cl^-)
Malic acid-water Tartaric acid-water Citric acid-water	Relative humidity	Malic acid (0–4.4 mol L^{-1}) Tartaric acid (0–4.2 mol L^{-1}) Citric acid (0–2.8 mol L^{-1})	Velezmoro and Meirelles (1998)	2%	Between groups in hydroxy-acids (CH_n, —COOH, and —OH) and water
Tartaric acid-NaCl-water	Activity coefficients at saturation of tartaric acid	NaCl (0–5.3 mol L^{-1})	Herz and Hiebenthal (1929)	53%	Between groups in hydroxy-acids (CH_n, —COOH and —OH) and ionic groups (Na^+ and Cl^-)
Diacid (C4-C13)-water	Activity coefficients at solubility of diacids	Diacids (0-solubility)	Acree (1991) Freier (1976)	20%	Between groups in diacids (—CH_n and —COOH) and water
Succinic acid-NaCl-water	Solubility of succinic acid	NaCl (0–5.3 mol L^{-1})	Herz (1909)	1%	Between groups in diacids (—CH_n and —COOH) and ionic groups (Na^+ and Cl^-)

*The sequence of correlations is the same as the order in which they are listed in this table.

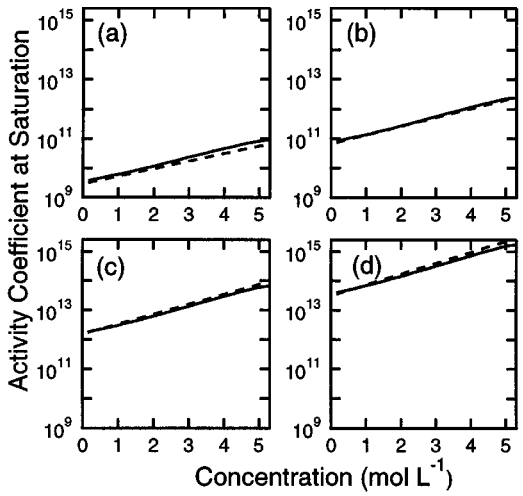

Figure 3. Activity coefficients at saturation in NaCl aqueous solution with four long-chain alkanes: (a) dodecane (C12), (b) tetradecane (C14), (c) hexadecane (C16), (d) octadecane (C18).

The correlation and empirical parameterization are represented by solid and dashed lines, respectively, in each panel. The empirical parameterization is taken from Sutton and Calder (1974).

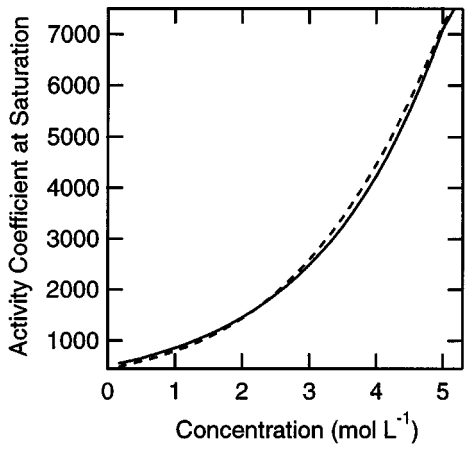

Figure 4. Activity coefficients at saturation in NaCl aqueous solution with hexanol.

The correlation and empirical parameterization are represented by solid and dashed lines, respectively. The empirical parameterization is taken from Zdenek et al. (1980).

dilution activity coefficients (IDACs) of alkanes, alcohols, acids, and ketones collected by Kojima et al. (1997) in Figure 2. In general, the compounds tend to have higher IDACs with increasing carbon numbers as indicated by UNIFAC-based models (Zhang et al., 1998). Our results agree well with the data, giving values within 8% of measured data for all four types of compounds. The IDACs of isomers that have the same carbon number, but different chemical structures, depend on the specific configurations of carbon chains, but cannot be predicted with the UNIFAC approach (Fredenslund et al., 1977).

The "salting-out" constants of NaCl with four long-chain alkanes including dodecane (C12), tetradecane (C14), hexadecane (C16), and octadecane (C18) were reported by Sutton and Calder (1974). Their activity coefficients at saturation for different concentrations of NaCl were calculated according to Eq. 29. From these data, the interaction parameters between ionic groups (Na^+ and Cl^-) and long-chain CH_n were fitted. The results are plotted in Figure 3. The "salting-out" effect causes the activity coefficients of organic solutes to increase with higher concentrations of NaCl. Consequently the compounds become less soluble with increasing salt concentration. At saturation for NaCl (about 5.3 mol·L^{-1}), the activity coefficients of four alkanes are normally 10 to 100 times larger than those in the absence of salt. The fitted correlations to measurements represent the general trend of the "salting-out" effect satisfactorily over much of the concentration range of NaCl, while deviations from experimental data are significant at the high concentration end. These errors are up to 30% in mixtures of alkanes with high NaCl concentrations (5.3 mol·L^{-1}), but the model agrees with the empirical parameterization within 10% at NaCl concentrations less than 2.0 mol·L^{-1}.

The "salting-out" constant of hexanol provided data for the dependence of activity coefficients of hexanol on NaCl concentration (Zdenek et al., 1980). The interaction parameters between NaCl and the long-chain —OH group were fitted from these data, as shown in Figure 4. The "salting-out" effect results in higher activity coefficients for the organic solute in increasingly concentrated salt solutions. With the solution saturated by NaCl, the activity coefficient of hexanol is approximately 8 times greater than that in pure water. The largest error of 5% occurs in the mixture of hexanol with a saturated NaCl concentration of 5.3 mol·L^{-1}. For salt concentrations lower than 2.5 mol·L^{-1}, the data correlations are within 3% of experimental measurements.

Multifunctional compounds

Glucose and fructose are two representative monosaccharide compounds for which a large amount of phase equilibrium data are available. The equilibrium relative humidity was measured at various concentrations of aqueous solution of glucose and fructose (Peres and Macedo, 1997). Two groups, alcohol (—OH) in monosaccharides and ether (—CH_nO) in monosaccharides, are introduced to represent their ring structure. Because of the large number of polar functional groups existing in the relatively short carbon chains of sugars, the carbon groups in this type of compounds are thought to be similar to those in short-chain monofunctional compounds, for example, ethanol and acetic acid. Since the interaction parameters involving CH_n groups in solutions containing short-chain monofunctional compounds have been well studied by LLE-UNIFAC (Magnussen et al., 1981), they are used to describe the carbons in short-chain multifunctional compounds. The correlations shown in Figure 5 are fitted directly to measurements to obtain each parameter. In the aqueous solution of glucose and fructose, the increasing concentrations of solutes lower the concentration of water, and thus the relative humidity. The highest concentrations of two organic solutes correspond to their respective solubility lim-

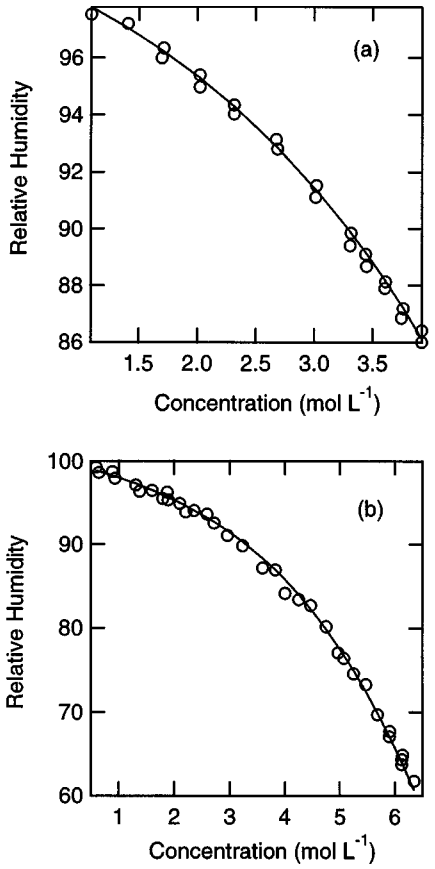

Figure 5. Relative humidity over aqueous solutions of (a) glucose and (b) fructose.

The correlation and experimental measurements are represented by a solid line and open circles, respectively. Experimental data are from Peres and Macedo (1997).

its. Because glucose (7 mol·kg^{-1}) is 50% less soluble than fructose (22 mol·kg^{-1}), these two compounds are used to represent low-solubility and high-solubility sugars, respectively. In Figure 5, the calculated relative humidities follow the measurements closely up to solubility limits. The results show that the same set of parameters are applicable to solutes of different solubilities. The errors associated with these correlations are less than 3%.

In hydroxy-acids including malic, tartaric and citric acids, multiple alcohol and carboxylic acid groups coexist in the same short carbon chain. Due to the high ratios of polar to nonpolar groups in diacids, special multifunctional groups, alcohol (—OH) and carboxylic acid (—COOH) in hydroxy-acid, are introduced to incorporate this type of compounds. LLE-UNIFAC parameters are used to describe the carbon groups present in hydroxy-acids. The correlations shown in Figure 6 are fitted to experimental data (Velezmoro and Meirelles, 1998) to obtain parmeters for hydroxy-acid interactions with water. The agreement between them is generally good for all three acids. The largest errors of 2% occur at high concentrations of malic and tartaric acid.

From enthalpy of melting and melting temperature data collected in Acree (1991), the fugacity ratios of a series of diacids (C4–C13 except C11) were calculated from Eq. 30. Using the limited solubility data of these compounds (Freier, 1976) in Eq. 29, we calculated the activity coefficient at saturation for each species from its known fugacity ratio and solubility. By using two new groups, methyl (CH_n) and carboxylic acid (—COOH) in diacids, the measured activity coefficients between 0.8 to 10^4 at saturation were fit as shown in Figure 7. The diacids with larger carbon numbers usually have higher coefficients, a trend shown more distinctly by the fitted correlation. Our correlations agree reasonably well with measurements over the broad range of carbon number of 4 to 13, with a mean deviation of 20%.

The solution system of glucose-NaCl-water and fructose-NaCl-water for different compositions and their corresponding relative humidities measured by Comesana et al. (1999) were used to fit interaction parameters between ionic groups and multifunctional groups in sugars (Figure 8). Figures 8a and 8b compare the correlations with the experimental results of relative humidity for these ternary systems. For the measured data points, the correlations of the experimental data have errors less than 0.1%. In Figures 8c and 8d, the data are reproduced with constant relative humidity isopleths and the measured values. Each line represents a series of concentrations of NaCl and organic solute that have the same relative humidity. The correlated relative humidity decreases

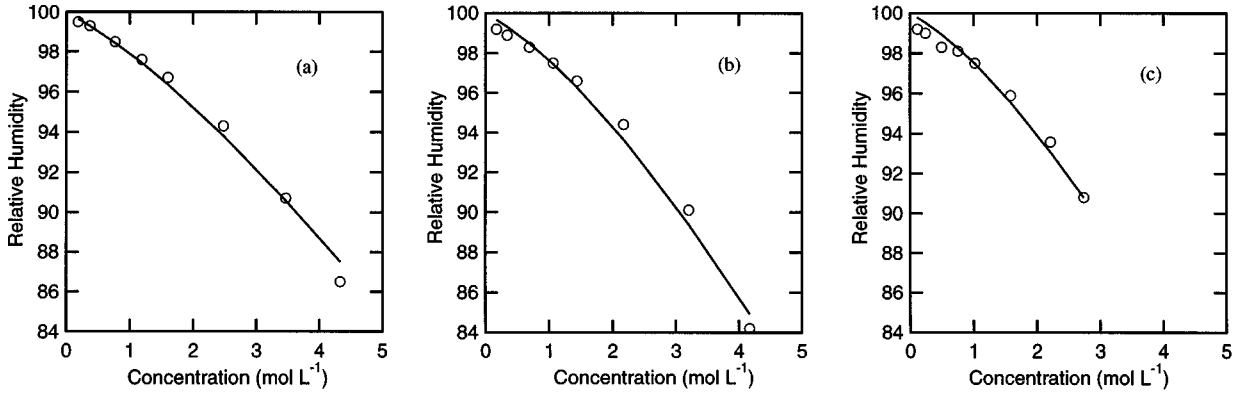

Figure 6. Correlated relative humidity over aqueous solutions of (a) malic acid, (b) tartaric acid, and (c) citric acid.

The correlation and experimental measurements are represented by solid line and open circles, respectively, in each panel. Experimental data are from Velezmoro and Meirelles (1998).

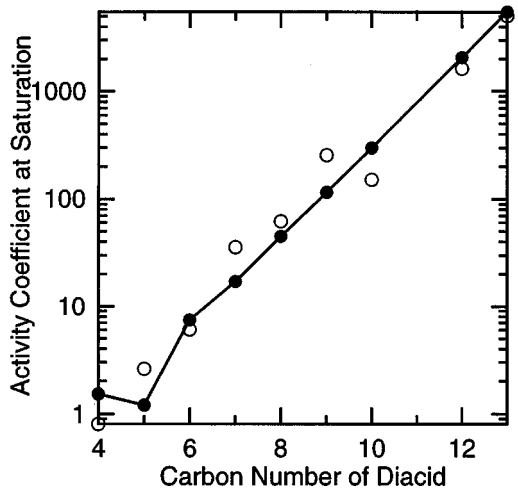

Figure 7. Activity coefficients at saturation in NaCl aqueous solution for a series of diacids.

The correlation and experimental measurements are represented by a solid line and open circles, respectively. Experimental data are from Acree (1991) and Freier (1976).

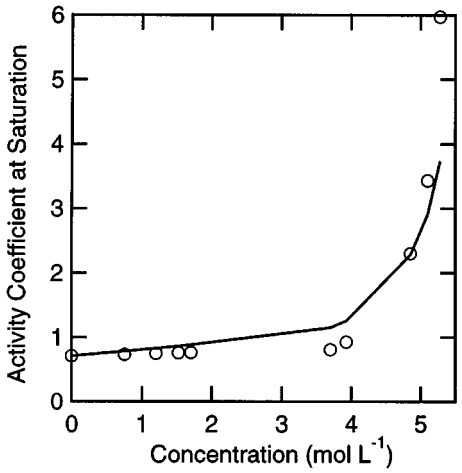

Figure 9. Activity coefficients at saturation in NaCl aqueous solution for tartaric acid.

The correlation and experimental measurements are represented by a solid line and open circles, respectively. Experimental data are from Herz and Hiebenthal (1929).

with increasing sugar and NaCl concentrations, corresponding within 0.1%. This type of simple two-parameter description of the interactions between electrolytes and organic species has also been used successfully to represent measured data by Clegg et al. (2001).

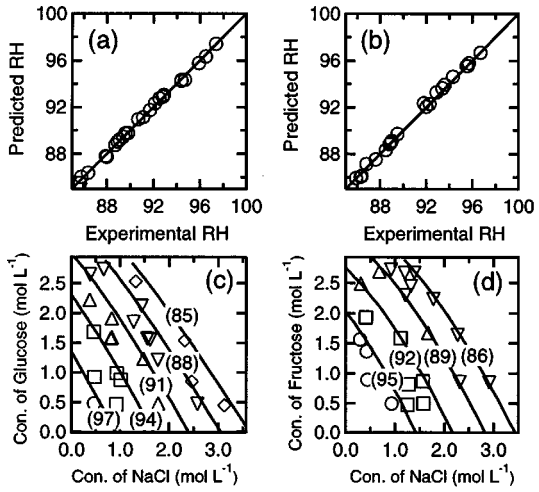

Figure 8. Relative humidity over solutions of glucose-NaCl-water and fructose-NaCl-water solutions.

Panels (a) and (b) are the direct comparison for glucose and fructose, respectively. In panels (c) and (d), the correlated lines of constant relative humidity are plotted with data points. Data are grouped according to their corresponding relative humidities. For glucose, five groups, 85%–88% (open diamonds), 88%–91% (open downward-pointing triangles), 91%–94% (open upward-pointing triangles), 94%–97% (open squares), and above 97% (open circles) are represented. For fructose, four groups, 86%–89% (open downward-pointing triangles), 89%–92% (open upward-pointing triangles), 92%–95% (open squares), and above 95% (open circles) are represented. Experimental data are from Comesana et al. (1999).

The activity coefficients of tartaric acid calculated from measured aqueous solubilities at different NaCl concentrations (Herz and Hiebenthal, 1929) were fit to interaction parameters between ionic groups and multifunctional groups in hydroxy-acids (Figure 9). The nonideality of the measured solutions is not well predicted by our correlations with average errors up to 53%, but the general trend is reproduced fairly well. More recent measurements of this system were not available to assess the reproducibility of the measurements.

Herz (1909) reported the variation of solubility of succinic acid with the concentration of NaCl aqueous solution. These data were used to fit interaction parameters between groups in diacids and ionic groups (Figure 10). The correlations for solubilities differ less than 1% from the measured solubilities.

Equilibrium Predictions

Water uptake by soluble components in aerosol results in a change in particle size depending on the relative humidity. In order to quantitatively describe the amount of water absorbed by particles, the hygroscopic growth factor (GF) is defined as the ratio of the diameter $D_{p,RH}$ at a specified relative humidity RH over the original dry diameter $D_{p,\mathrm{dry}}$ (measured at a relative humidity that is predicted to be below the efflorescence humidity of all solutes present) (Hämeri et al., 2000)

$$GF(RH) = \frac{D_{p,RH}}{D_{p,\mathrm{dry}}} \tag{34}$$

The relative humidity (RH) at equilibrium is related to the activity of water as

$$RH = 100 x_w \gamma_w \tag{35}$$

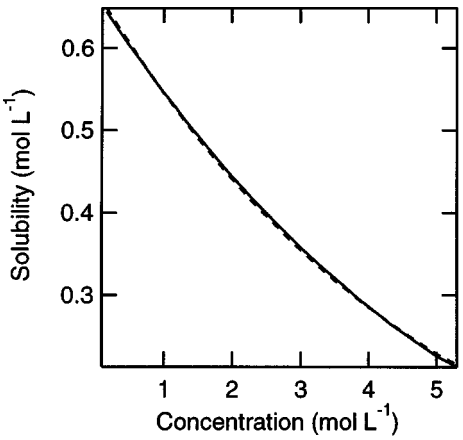

Figure 10. Solubility in NaCl aqueous solution for succinic acid.

The model correlation and empirical parameterization are represented by solid and dashed lines, respectively. The empirical parameterization is from Herz (1909).

in the bulk solution where the influence of interfacial energy is negligible. For particles smaller than 50 nm in diameter, the Kelvin effect makes the relative humidity at equilibrium higher than the water activity of the aerosol solution.

The hygroscopic growth factors of marine aerosol have been measured in several field campaigns (Berg et al., 1998; Swietlicki et al., 2000; Zhou et al., 2001). Ming and Russell (2001) present growth factors of sea salt aerosol calculated at various organic contents and initial dry particle sizes using the estimated sea salt particle chemical compositions and comparisons of the model predictions with field measurements. To study the influence of organic compounds of different solubilities on water uptake, we compare here hygroscopic properties of relatively simple mixed ion-organic aerosol predicted by our model to published laboratory measurements (Hämeri et al., 2002; Cruz and Pandis, 2000). In this study, the aerosol is formed by mixing one of three diacids (malonic acid, succinic acid, and glutaric acid) with an inorganic salt (either NaCl or $(NH_4)_2SO_4$) at different ratios. The presence of this type of diacid in the atmosphere has been observed by Kawamura et al. (1990). The aqueous solubilities and other chemical information of these compounds are listed in Table 3. Malonic acid and glutaric acid are highly soluble, while succinic acid is only slightly soluble. These three compounds are used as representatives of the soluble (solubility greater than 3 mol L^{-1}) and insoluble (solubility less than 1 mol L^{-1}) organic species present in aerosol particles. Since measured salting-out constants of organic species in $(NH_4)_2SO_4$ solutions are not available, we cannot correlate the interaction parameters of NH_4^+ and SO_4^{2+} with organic groups. Consequently, we have resorted to assuming that their salting-out behavior is similar to Na^+ and Cl^-. Since this assumption is likely to be inaccurate, we estimated the error introduced in this assumption by also assuming no NH_4^+-organic and no SO_4^{2+}-organic interactions (as discussed in the section on model sensitivity). Further refinement of the model to include data for $(NH_4)_2SO_4$ or more similar compounds salting-out constants may improve the model significantly when those data are available.

Table 3. Properties of Inorganic and Organic Compounds Studied in this Work

Compounds	Molecular Wt. (mol^{-1})	Solubility ($mol \cdot L^{-1}$) at 298.15 K	Density ($g \cdot cm^{-3}$)
NaCl	58.44 †	4.53 †	2.17 †
$(NH_4)_2SO_4$	132.14 †	3.28 †	1.77 †
Malonic acid	104.06 †	5.98 *	1.62 †
Succinic acid	118.09 †	0.68 *	1.55 †
Glutaric acid	132.11 †	4.07 *	1.42 †

*Saxena and Hildemann (1996).
†Lide (2000).

Pure substances

The predicted hygroscopic growth curves of pure NaCl and $(NH_4)_2SO_4$ are plotted in Figure 11. In aqueous solutions only containing electrolytes, our results reduce to the Pitzer-Simonson-Clegg model, which was shown to represent the experimental data of aqueous solutions of NaCl and $(NH_4)_2SO_4$ within 1% accuracy (Clegg et al., 1992, 1998). The growth factors of particles composed of pure NaCl and pure $(NH_4)_2SO_4$ as measured by Cruz and Pandis (2000) and Hämeri et al. (2002) are included in Figure 11. The measured deliquescence relative humidity (DRH) of each salt agrees with theoretical values (NaCl at 75%; $(NH_4)_2SO_4$ at 80%), although the measured deliquescence processes are not as sharp as predicted. Above the DRH, the particles are pre-

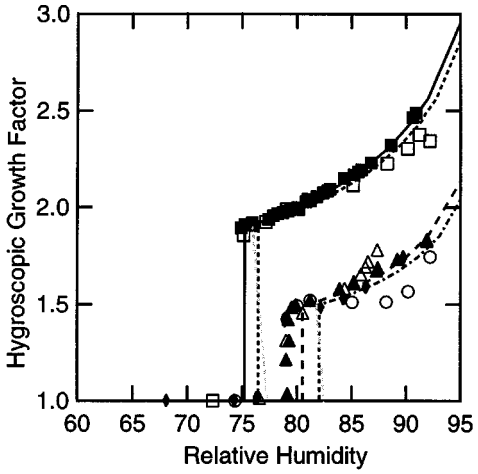

Figure 11. Predicted and measured hygroscopic growth curves of particles composed of pure NaCl (solid line for bulk case; dotted line for dry diameter of 100 nm) and pure $(NH_4)_2SO_4$ (dashed line for bulk case; dashed-dotted line for dry diameter of 100 nm).

The experimental data are from Tang et al. (1986) (solid square for NaCl of bulk case), Tang and Munkelwitz (1994) (solid triangle for $(NH_4)_2SO_4$ of bulk case), Cruz and Pandis (2000) (open square for NaCl of dry diameter of 100 nm; open circle for $(NH_4)_2SO_4$ of dry diameter of 100 nm), Hämeri et al. (2000) (solid diamond for $(NH_4)_2SO_4$ of dry diameter of 50 nm) and Hämeri et al. (2002) (open triangle for $(NH_4)_2SO_4$ of dry diameter of 100 nm). For curves with multiple equilibria near deliquescence, shaded lines show the deliquescence path and shaded dotted lines show unstable equilibria.

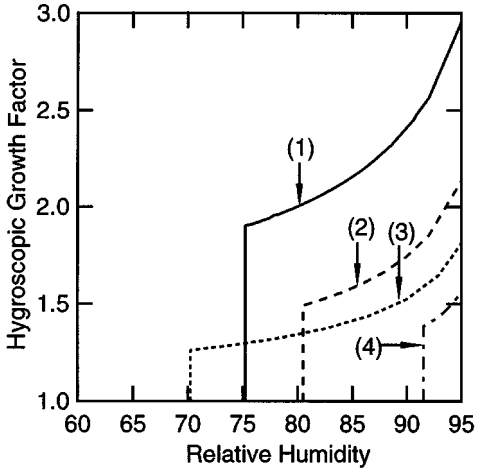

Figure 12. Predicted hygroscopic growth of particles composed of pure substances.

(1) Solid line for NaCl; (2) dashed line for $(NH_4)_2SO_4$; (3) dotted line for malonic acid; (4) dashed-dotted line for glutaric acid.

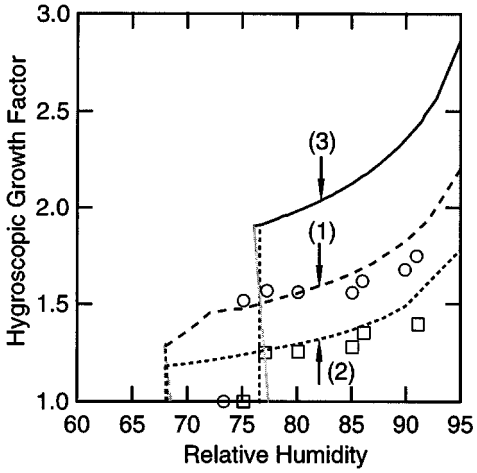

Figure 13. Predicted hygroscopic growth of particles (dry diameter 100 nm) with varying organic compositions.

The two compositions studied are: (1) 50% NaCl and 50% glutaric acid (model prediction: dashed line; experimental measurements: open circle); (2) 80% NaCl and 20% glutaric acid (model prediction: dotted line; experimental measurements: open square); and (3) 100% NaCl (solid line) is included for reference. Experimental data are from Cruz and Pandis (2000).

dicted to experience smooth growth with increasing relative humidity. However, the measurements of Cruz and Pandis (2000) of $(NH_4)_2SO_4$ differ from those of Hämeri et al. (2002) between relative humidities of 85% and 99% by between 20% and 30%. The strictly inorganic salt hygroscopic growth studies of Hämeri et al. (2000) show better agreement at these high relative humidities for the pure salt cases. The predicted hygroscopic growth of $(NH_4)_2SO_4$ lies between these two measurements for this humidity range.

Predictions for malonic acid and glutaric acid indicate deliquescence at 70% and 92%, respectively, while succinic acid does not take up water until 99% (Figure 12). By constraining the model with solubility data listed in Table 3, the compounds with higher solubility generally tend to deliquesce at lower relative humidity, lowering the predicted DRH. The DRH of glutaric acid measured by Cruz and Pandis (2000) is $85\% \pm 5\%$, roughly consistent with the model prediction.

NaCl with 50% glutaric acid (base case)

The DRH of glutaric acid is between those of malonic acid and succinic acid. Aerosol particles consisting of internally mixed NaCl and glutaric acid each accounted for half of the total dry mass in the base case in this study. In Figure 13, the predicted hygroscopic growth curve of the base case at dry initial diameter of 100 nm together with the measurements by Cruz and Pandis (2000) is compared with the pure NaCl case. Mixing with glutaric acid decreases the DRH of NaCl from 75% to 68% according to the model prediction, whereas the experiments indicate a decrease of less than 3%. At deliquescence, glutaric acid is completely dissolved, while only part of NaCl is dissolved. After that, the remaining NaCl continues to dissolve and results in almost linear growth with relative humidity between 68% and 72%. After all NaCl dissolves at 72%, the particles grow smoothly with increasing relative humidity. Although the predicted phenomenon of decreased DRH due to mixing with organic species was not observed by Cruz and Pandis (2000), other observational and modeling studies agree with this prediction (Andrews and Larson, 1993; Hansson et al., 1998; Wexler and Seinfeld, 1991). Despite the discrepancy in DRH, the measured growth factors between 75% and 90% relative humidity match the prediction. Compared with the pure NaCl case, the presence of 50% glutaric acid shows a decrease of 30% in growth at relative humidities above 75%, while significant growth occurs between 68% and 75% as a result of decreased DRH.

Varied organic fractions

The fraction of the total aerosol mass occupied by glutaric acid is increased to 80% to study the impact of the organic fraction on hygroscopic growth. The predicted growth curve and measured data points are shown together with the base case of 50% glutaric acid in Figure 13. Since the DRH is independent of the relative fractions of components, deliquescence still occurs at 68%. However, the increased organic fraction further decreases the growth as compared to the base case. In general, the hygroscopic growth decreased 65% relative to the pure NaCl. In the relative humidity range between 75% and 90%, the predictions and measurements agree within 20%.

Particle-size variation

The growth curves for the base case composition (50% NaCl and 50% glutaric acid) with 15 nm, 35 nm, 50 nm, 75 nm, 100 nm, and 165 nm dry diameter are compared with the bulk case in Figure 14. Surface tension decreases the hygroscopic growth by 3% at 100 nm, 4% at 50 nm, 10% at 65 nm, and

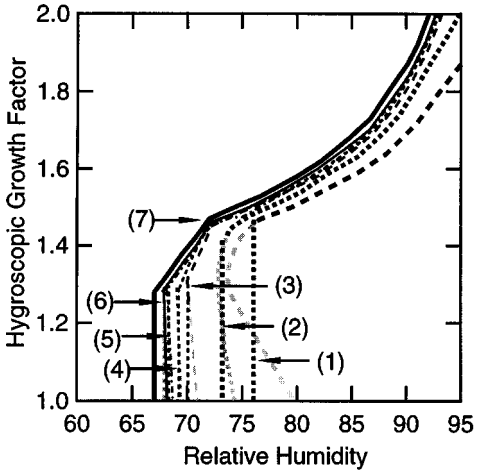

Figure 14. Influence of surface tension on hygroscopic growth of 50% NaCl and 50% glutaric acid.

The initial dry diameters studied are: (1) 15 nm (thick dotted line); (2) 35 nm (thick dashed line); (3) 50 nm (dashed line); (4) 75 nm (dotted line); (5) 100 nm (dashed-dotted line); (6) 165 nm (solid line); and (7) bulk case (thick solid line).

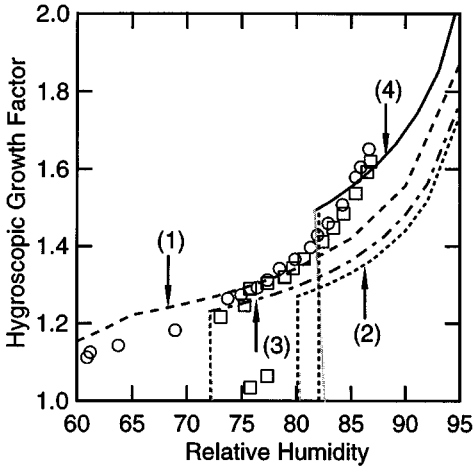

Figure 15. Predicted hygroscopic growth of particles (dry diameter 100 nm) with varying compositions.

The compositions studied are: (1) 50% $(NH_4)_2SO_4$ and 50% malonic acid (model prediction: dashed line; experimental measurements: open circles); (2) 50% $(NH_4)_2SO_4$ and 50% succinic acid (model prediction: dashed line; experimental measurements: open squares); (3) 50% $(NH_4)_2SO_4$ and 50% glutaric acid (model prediction: dashed-dotted line); and (4) 100% $(NH_4)_2SO_4$ (solid line). Experimental data are from Hämeri et al. (2002).

20% at 15 nm relative to the bulk case. The presence of negatively-sloped deliquescence regions in the smallest particle sizes results from surface tension effects and is discussed in Russell and Ming (2002).

$(NH_4)_2SO_4$ with organic acids

In Figure 15, the predicted hygroscopic growth curves of three mixtures (50% $(NH_4)_2SO_4$ with 50% malonic acid, $(NH_4)_2SO_4$ with 50% succinic acid, and 50% $(NH_4)_2SO_4$ with 50% glutaric acid) are plotted together with measurements. The inclusion of malonic acid lowers the DRH of pure $(NH_4)_2SO_4$ from 80% to 58%. Hämeri et al. (2002) reported that the particles of this composition grew continuously with increasing relative humidity from 62%. Good agreement between predicted and measured growth occurs in the relative humidity range from 60% to 80%. As in the pure $(NH_4)_2SO_4$ case, the predicted growth is less than the measurements above 80%. The predicted DRH of $(NH_4)_2SO_4$ with 50% succinic acid remains at 80% since the solubility of succinic acid is small. At the relative humidity above 80%, the predicted growth is well below measurements. Similar to malonic acid, glutaric acid is also able to decrease the DRH of $(NH_4)_2SO_4$ from 80% to 72%. Above 80%, its growth is slightly higher than succinic acid and significantly lower than malonic acid. Although the presence of all three diacids lowers the water uptake after 80%, the particles containing the more soluble organic species tend to grow bigger than those with the less soluble species. The model predicts that the presence of 50% malonic acid decreases the growth by 20% relative to pure $(NH_4)_2SO_4$, while 50% glutaric acid and 50% succinic acid cause decreases of 35% and 38%, respectively.

Model Sensitivity

To assess the sensitivity of the model to the many empirical parameterizations that we have employed, we compare here a series of different approaches to our most important assumptions, namely the organic-ion interaction parameters, interactions between $(NH_4)_2SO_4$ and organics, internal and external mixing states, and empirical correlations of diacids.

Organic-ion interaction parameters

In the calculation of organic-ion interaction parameters for UNIFAC, the volume and area parameters R_i and Q_i of ion i in Eq. 4 of Fredenslund et al. (1975) are arbitrarily set to be equal to those of water. Hence, the combinatorial contribution to activity coefficient reduces to zero for inorganic-only aqueous solutions. Because the Pitzer-Simonson-Clegg model solely determines the properties of such solutions, the predictive accuracy of our model is the same as the Pitzer-Simonson-Clegg model that has been well developed for inorganic solutions. Macedo et al. (1990) suggested treating R_i and Q_i as adjustable parameters and fitting them to experimental data. The Kikic et al. (1991) model used the R_i and Q_i values given by Macedo et al. (1990). Figure 16 compares these alternative parameterizations to our approach of setting them equal to those of water.

In Figure 16, the hygroscopic growth curves of pure NaCl predicted in two cases are compared with experimental data (Tang et al., 1986). Using identical values of R_i and Q_i as for water cancels the combinatorial contribution to the overall activity coefficients. Our model fully accounts for the growth and compares well with measurements. In the Macedo et al. (1990) approach, the non-zero combinatorial contribution shifted the predicted DRH of pure NaCl to 80%. At relative humidities higher than DRH, the growth predicted by this approach is 5% lower than our model and the measurements of Tang et al. (1986).

The ability of different R_i and Q_i values to also represent the "salting-out" effect is illustrated in Figure 17. Both types

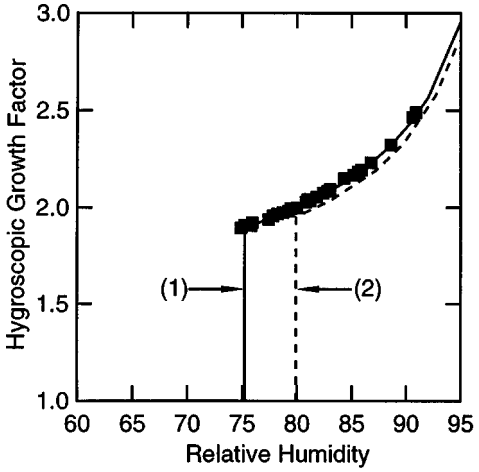

Figure 16. Predicted and measured hygroscopic growth curves of particles (dry diameter 100 nm) composed of pure NaCl.

The predictions show: (1) this work (solid line); and (2) Macedo et al. (1990) (dashed line). Data (solid square) are from Tang et al. (1986).

of parameters are able to correlate the general trend of solubility of succinic acid in NaCl aqueous solution. Our correlation agrees with measurements generally within 2%, while using the parameters given by Macedo et al. (1990) results in an average deviation of 6%.

The hygroscopic growth curves of particles with a composition of 50% NaCl and 50% glutaric acid are calculated from the interaction parameters fitted from solubility data. With the Macedo et al. (1990) parameters, the mixture deliquesces at a relative humidity of 77%, slightly higher than that of pure NaCl (75%), as shown in Figure 18.

Interactions between $(NH_4)_2SO_4$ and organics

In the previous calculations, the interaction parameters of NH_4^+ and SO_4^{2-} with organic groups are replaced by those of

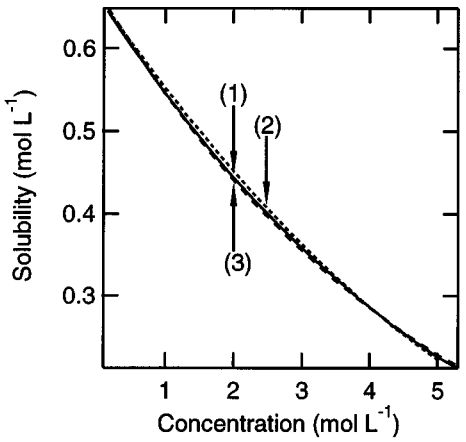

Figure 17. Predicted solubility in NaCl aqueous solution with parameterized experimental measurements for succinic acid.

The predictions are based on: (1) this work (dashed line); and (2) Macedo et al. (1990) (dotted line). Experimental data (3, solid line) are from Herz and Hiebenthal (1929).

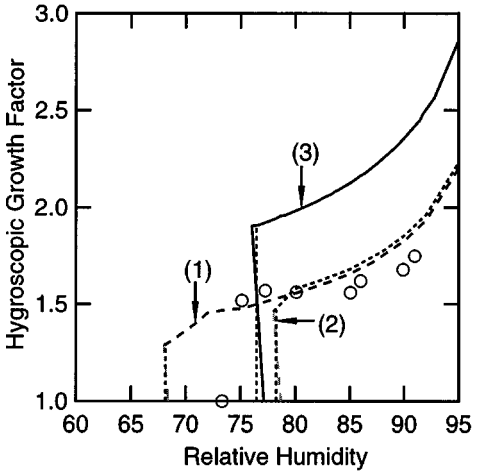

Figure 18. Predicted hygroscopic and measured hygroscopic growth curves of particles (dry diameter 100 nm) of 50% NaCl and 50% glutaric acid.

The curves illustrate: (1) model predicted mixture behavior from this work (dashed line); and (2) Macedo et al. (1990) (dotted line); and (3) pure NaCl. Data (open circles) are from Cruz and Pandis (2000).

Na^+ and Cl^-. In order to test the uncertainty caused by this assumption on hygroscopic growth, we recalculate the growth curve of 50% glutaric acid with 50% $(NH_4)_2SO_4$ by assuming no interaction and doubling the interaction between them and comparing to the growth curve with interaction in Figure 19. In general, the interaction between $(NH_4)_2SO_4$ and glutaric acid assists the water uptake. The growth without interaction is 10% lower than that with interaction; doubling the strength of the interaction results in a 10% increase in the growth factor. The elimination of ion-organic interaction also re-

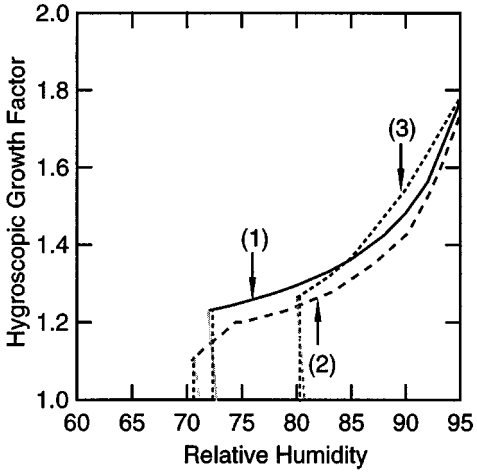

Figure 19. Influence of interaction between $(NH_4)_2SO_4$ and organic compounds on hygroscopic growth of 50% $(NH_4)_2SO_4$ and 50% glutaric acid.

Predictions were calculated: (1) with interaction (solid line); (2) without interaction (dashed line); and (3) with interaction twice as strong as NaCl (dotted line).

duces the DRH to 71%, while the DRH remains at 80% with doubling the strength.

Internal and external mixing states

In the previous model calculation, we assume that the inorganic and organic components in aerosol are internally mixed. Compared to the pure salt case, mixing with organic compounds decreases water uptake at relative humidities above the DRH. In addition, the soluble organic compounds lower the mixture DRH from that of the pure salt and result in considerable growth at low relative humidities. Since measurements suggest that particles often exist in external mixtures, we study here the influence of mixing state on hygroscopic growth.

The normalized water content (WC) is defined as the ratio of the mass of absorbed water in particles $m_{w,RH}$ at a specific relative humidity RH over the total dry particle mass $m_{p,\mathrm{dry}}$

$$WC(RH) = \frac{m_{w,RH}}{m_{p,\mathrm{dry}}} \tag{36}$$

The average water content of an externally mixed aerosol is defined as

$$WC(RH) = \epsilon_O WC_O(RH) + (1-\epsilon_O) WC_S(RH) \tag{37}$$

where $WC_O(RH)$ and $WC_S(RH)$ are the water contents of a pure organic compound and salt at relative humidity RH, respectively, and ϵ_O is the organic mass fraction in the dry particle. The average water content for particles of four different compositions is calculated by assuming external mixing, and the results are compared with the respective internal cases in Figure 20. In the externally mixed case, the DRH of each component is unchanged from its pure value. Therefore, there is no growth until the relative humidity increases to the lowest DRH of all pure components. Each component begins to contribute to the overall growth only when its DRH is reached. For particles containing soluble compounds such as malonic acid and glutaric acid, the external growth is less than internal growth before the organic component is dissolved. After the dissolution of the organic component, the externally mixed aerosol grows more than the internally mixed one. In the case of the low-solubility succinic acid, the external growth is approximately the same as the internal growth, since the DRH of succinic acid is higher than 99%. The largest deviation of 10% between internal and external growth is observed in the case containing the highly soluble species malonic acid. For less soluble succinic acid and glutaric acid, the two types of growth generally agree within 3%.

Empirical correlations of diacids

The uncertainties of the measurements used for model parameterization result in analogous uncertainties in the model calculations. Since experimental errors can be propagated in our calculation, the individual model parameters were varied to quantify the resulting errors associated with the predicted hygroscopic growth factors.

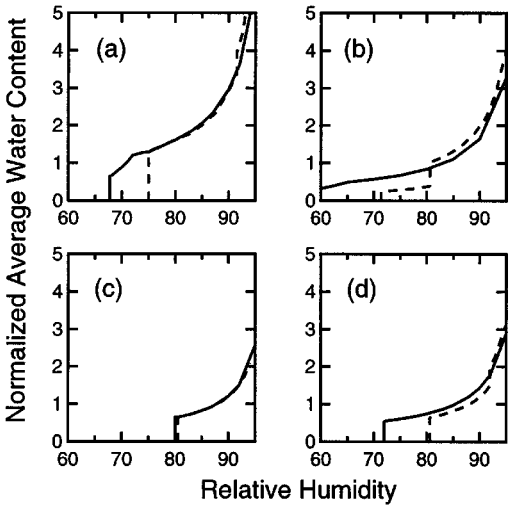

Figure 20. Predicted average water contents of particles by assuming internal (solid line) and external (dashed line) mixing for: (a) 50% NaCl and 50% glutaric acid, (b) 50% $(NH_4)_2SO_4$ and 50% malonic acid, (c) 50% $(NH_4)_2SO_4$ and 50% succinic acid, and (d) 50% $(NH_4)_2SO_4$ and 50% glutaric acid.

The model sensitivity to the interaction parameters involving monofunctional compounds, sugars and hydroxy-acids has been examined by Ming and Russell (2001). Two other types of interactions used in the base case (50% NaCl with 50% glutaric acid) are (1) interactions between diacids and water and (2) interactions between diacids and electrolytes. The sensitivity of the base case calculation is summarized in Table 4. At two representative relative humidities 73% and 85%, the change in the calculated hygroscopic growth factors caused by error in experimental data used is less than 1%.

Conclusions

A thermodynamic model was developed to describe the phase equilibria of electrolyte-organic mixtures in aerosol particles. Three types of contributions to activity coefficients including ion-water, organic-water, and ion-organic interactions are accounted for by combining the Pitzer-Simonson-Clegg model and the UNIFAC framework into a general model. The model is parameterized by fitting interaction parameters from experimental data collected in the literature. The accuracy of the model correlations compare well with available measurements. The hygroscopic growth curves calculated by the model achieve good agreement with measurements (Cruz and Pandis, 2000; Hämeri et al., 2001). The results show that the water uptake by ion-organic mixtures is influenced by the solubility of organic compounds. The presence of 50% malonic acid in $(NH_4)_2SO_4$ reduces the growth by 20%, while a 30% decrease is incurred by 50% succinic acid. The soluble organic compounds can also decrease the DRH of pure salt. The model predicts that mixing with 50% malonic acid lowers the DRH of $(NH_4)_2SO_4$ from 80% to 58%.

The approach of treating the volume and area parameters in UNIFAC as adjustable (Kikic et al., 1991) shifted the pre-

Table 4. Sensitivity of Model Predictions to Experimental Uncertainty in Data Used in Empirical Correlations

Parameters in Model	Type of Input Data	Uncertainty of Input Data	Sensitivity* of Growth Factor at 73% (85%†)
Volume and area parameters for organic-ion interactions	Parameters fitted from experimental data (Macedo et al., 1990)	±50%	$(1.656 \pm 0.003^{+\ddagger})$
Salting-out effect of NH_4^+ and SO_4^{2-}	Solubility of succinic acid in NaCl aqueous solution (Herz, 1909)	±5%	$1.155 \pm 0.085^{\ddagger}$ (1.306 ± 0.063)
External mixtures	Field measurements (Middlebrook et al., 1998)	100% external, 100% internal	$(1.656 \pm 0.001^{\dagger})$
Interaction parameters between CH_n and H_2O in diacids	Activity coefficients at saturation (Acree, 1991; Freier, 1976)	±50%	1.462 ± 0.008 (1.656 ± 0.003)
Interaction parameters between ions and groups in diacids	Solubility of succinic acid in NaCl aqueous solution (Herz, 1909)	±5%	1.462 ± 0.014 (1.656 ± 0.012)

* ± Variation represents the sensitivity of the prediction to the uncertainty in the experimental data used in the correlation of model parameters.
†Uncertainty is given at 85% relative humidity because 73% is below the deliquescence relative humidity.
‡The growth factors and associated uncertainties are calculated for 50% $(NH_4)_2SO_4$ and 50% glutaric acid.

dicted DRH of pure NaCl to 80%, as opposed to 75% predicted by our model and measured by Tang et al. (1986). Doubling the ion-organic interaction between $(NH_4)_2SO_4$ and glutaric acid increases, and eliminating them lowers, the hygroscopic growth factor by 10%. Comparisons of the growth curves of internally and externally mixed aerosol indicate that the DRH of an internal mixture is lower than that of an external mixture, and the external mixture grows over 3% more than the internal mixture after all soluble components are dissolved. The change in the hygroscopic growth factors caused by errors in experimental data used in the model parameterization is less than 1%.

Acknowledgments

This analysis was supported under Office of Naval Research grants N00014-97-1-0673 and N00014-98-1-0565. The authors are grateful to Simon Clegg, John Prausnitz, Stanley Sandler, and their research groups for helpful discussions about this work.

Literature Cited

Acree, W. E., "Thermodynamic Properties of Organic Compounds: Enthalpy of Fusion and Melting Point Temperature Compilation," *Thermochimica Acta*, **189**, 37 (1991).

Ansari, A. S., and S. N. Pandis, "Water Adsorption by Secondary Organic Aerosol and Its Effects on Inorganic Aerosol Behavior," *Environ. Sci. Technol.*, **34**, 71 (2000).

Andrews, E., and S. M. Larson, "Effect of Surface Layers on the Size Changes of Aerosol-Particles as a Function of Relative-Humidity," *Environ. Sci. Technol.*, **27**, 857 (1993).

Ansari, A. S., and S. N. Pandis, "Water Absorption by Secondary Organic Aerosol and Its Effect on Inorganic Aerosol Behavior," *Environ. Sci. Technol.*, **34**, 71 (2000).

Bastos, J. C., M. E. Soares, and A. G. Medina, "Infinite Dilution Activity Coefficients Predicted by UNIFAC Group Contribution," *Ind. Eng. Chem. Res.*, **27**, 1269 (1988).

Berg, O. H., E. Swietlicki, and R. Krejci, "Hygroscopic Growth of Aerosol Particles in the Marine Boundary Layer over the Pacific and Southern Oceans During the First Aerosol Characterization Experiment (ACE 1)," *J. Geophys. Res.*, **103**, 16535 (1998).

Clegg, S. L., K. S. Pitzer, and P. Brimblecombe, "Thermodynamics of Multicomponent, Miscible, Ionic-Solutions: 2. Mixtures Including Unsymmetrical Electrolytes," *J. Phys. Chem.*, **96**, 9470 (1992).

Clegg, S. L., K. S. Pitzer, and P. Brimblecombe, "Correction," *J. Phys. Chem.*, **98**, 1368 (1994).

Clegg, S. L., K. S. Pitzer, and P. Brimblecombe, "Correction," *J. Phys. Chem.*, **99**, 6755 (1995).

Clegg, S. L., P. Brimblecombe, and A. S. Wexler, "Thermodynamic Model of the System H^+-NH_4^+-Na^+-SO_4^{2-}-NO_3^--Cl^--H_2O at 298.15 K," *J. Phys. Chem. A.*, **102**, 2155 (1998).

Clegg, S. L., J. H. Seinfeld, and P. Brimblecombe, "Thermodynamic Modelling of Aqueous Aerosols Containing Electrolytes and Dissolved Organic Compounds," *J. Aerosol Sci.*, **32**, 713 (2001).

Comesana, J. F., A. Correa, and K. Sereno, "Measurements of Water Activity in 'Sugar' Plus Sodium Chloride Plus Water Systems at 25 Degrees C," *J. Chem. Eng. Data*, **44**, 1132 (1999).

Corrigan, C. E., and T. Novakov, "Cloud Condensation Nucleus Activity of Organic Compounds: A Laboratory Study," *Atmos. Environ.*, **33A**, 2661 (1999).

Cruz, C. N., and S. N. Pandis, "A Study of the Ability of Pure Secondary Organic Aerosol to Act as Cloud Condensation Nuclei," *Atmos. Environ.*, **31A**, 2205 (1997).

Cruz, C. N., and S. N. Pandis, "Deliquescence and Hygroscopic Growth of Mixed Inorganic-Organic Atmospheric Aerosol," *Environ. Sci. Technol.*, **34**, 4313 (2000).

Duce, R. A., V. A. Mohnen, P. R. Zimmerman, D. Grosjean, W. Cautreels, R. Chatfield, R. Jaenicke, J. A. Ogren, E. D. Pellizzari, and G. T. Wallace, "Organic Material in the Global Troposphere," *Rev. Geophys.*, **21**, 921 (1983).

Fredenslund, A., J. Gmehling, and P. Rasmussen, *Vapor-Liquid Equilibrium Using UNIFAC*, Elsevier, Amsterdam (1977).

Fredenslund, A., R. L. Jones, and J. M. Prausnitz, "Group-Contribution Estimation of Activity Coefficients in Nonideal Liquid Mixtures," *AIChE J.*, **21**, 1086 (1975).

Freier, R. K., *Aqueous Solutions Data for Inorganic and Organic Compounds*, W. De Gruyter, New York (1976).

Gagosian, R. B., E. T. Peltzer, and O. C. Zafiriou, "Atmospheric Transport of Continentally Derived Lipids to the Tropical North Pacific," *Nature*, **291**, 312 (1981).

Gmehling, J., P. Rasmussen, and A. Fredenslund, "Vapor-Liquid Equilibria by UNIFAC Group Contribution. Revision and Extension: 2," *Ind. Eng. Chem. Process Des. Dev.*, **21**, 118 (1982).

Gmehling, J., "From UNIFAC to Modified UNIFAC to PSRK with the Help of DDB," *Fluid Phase Equilibr.*, **107**, 1 (1995).

Gogou, A. I., M. Apostolaki, and E. G. Stephanou, "Determination of Organic Molecular Makers in Marine Aerosols and Sediments: One-Step Flash Chromatography Compound Class Fractionation and Capillary Gas Chromatograph Analysis," *J. Chromatogr. A*, **799**, 215 (1998).

Hämeri, K., R. Charlson, and H. C. Hansson, "Hygroscopic Properties of Particles Containing Ammonium Sulphate Mixed with Carboxylic Acids," *AIChE J.*, in press (2002).

Hämeri, K., M. Väkevä, H. C. Hansson, and A. Laaksonen, "Hygroscopic Growth of Ultrafine Ammonium Sulfate Aerosol Measured Using a Ultrafine Tandem Differential Mobility Analyzer," *J. Geophys. Res.*, **105**, 22231 (2000).

Hansson, H. C., M. J. Rood, S. Koloutsou-Vakakis, K. Hämeri, D. Orsini, and A. Wiedensohler, "NaCl Aerosol Particle Hygroscopicity Dependence on Mixing with Organic Compounds," *J. Atmos. Chem.*, **31**, 321 (1998).

Herz, W., "Ein Beispiel von Löslichkeitsbeeinflussung," *Z. anorg. Chem.*, **65**, 341 (1909).
Herz, W., and F. Hiebenthal, "Über Löslichkeitsbeeinflussungen," *Z. anorg. allgem. Chem.*, **177**, 363 (1929).
Kawamura, K., and R. B. Gagosian, "Midchain Ketocarboxylic Acids in the Remote Marine Atmosphere—Distribution Patterns and Possible Formation Mechanisms," *J. Atmos. Chem.*, **11**, 107 (1990).
Kikic, I., M. Fermeglia, and P. Rasmussen, "UNIFAC Prediction of Vapor-Liquid Equilibrium in Mixed Solvent-Salt Systems," *Chem. Eng. Sci.*, **46**, 2775 (1991).
Köhler, H., "Zur Kondensation des Wasserdampfe in der Atmoshpäre," *Geofys. Publ.*, **2**, 3 (1921).
Kojima, K., S. Zhang, and T. Hiaki, "Measuring Methods of Infinite Dilution Activity Coefficients and a Database for Systems Including Water," *Fluid Phase Equilib.*, **131**, 145 (1997).
Laaksonen, A., "The Composition Size Dependence of Aerosols Created by Dispersion of Surfactant Solutions," *J. Colloid Interf. Sci.*, **159**, 517 (1993).
Li, J. D., H. M. Polka, and J. Gmehling, "A G(E) Model for Single and Mixed-Solvent Electrolyte System. 1. Model and Results for Strong Electrolytes," *Fluid Phase Equilib.*, **94**, 89 (1994).
Li, Z. B., Y. G. Li, and J. F. Lu, "Surface Tension Model for Concentrated Electrolyte Aqueous Solutions by the Pitzer Equation," *Ind. Eng. Chem. Res.*, **38**, 1133 (1999).
Lide, D. R., ed., *CRC Handbook of Chemistry and Physics*, CRC Press, Boca Raton, FL (2000).
Long, F. A., and W. F. McDevit, "Activity Coefficients of Nonelectrolyte Solutes in Aqueous Salt Solutions," *Chem. Rev.*, **51**, 119 (1952).
Macedo, E., P. Skovborg, and P. Rasmussen, "Calculation of Phase Equilibria for Solutions of Strong Electrolytes in Solvent-Water Mixtures," *Chem. Eng. Sci.*, **45**, 875 (1990).
Magnussen, T., P. Rasmussen, and A. Fredenslund, "UNIFAC Parameter Table for Prediction of Liquid-Liquid Equilibria," *Ind. Eng. Chem. Process Des. Dev.*, **20**, 331 (1981).
Meng, Z. Y., J. H. Seinfeld, P. Saxena, and Y. P. Kim, "Atmospheric Gas–Aerosol Equilibrium: 4. Thermodynamics of Carbonates," *Aerosol Sci. Technol.*, **23**, 131 (1995).
Middlebrook, A. M., D. M. Murphy, and D. S. Thomson, "Observations of Organic Material in Individual Marine Particles at Cape Grim During the First Aerosol Characterization Experiment (ACE 1)," *J. Geophys. Res.*, **103**, 16475 (1998).
Ming, Y., and L. M. Russell, "Predicted Hygroscopic Growth of Sea Salt Aerosol," *J. Geophys. Res.*, **106**, 28259 (2001).
Mirabel, P., H. Reiss, and R. K. Bowles, "A Theory for the Deliquescence of Small Particles," *J. Chem. Phys.*, **113**, 8200 (2000).
More, J. J., B. S. Garbow, and K. E. Hillstrom, *User Guide for MINPACK-1*, Argonne National Laboratory, Argonne, IL (1980).
Nath, S., "Surface Tension of Nonideal Binary Liquid Mixtures as a Function of Composition," *J. Colloid Interf. Sci.*, **209**, 116 (1999).
Park, J. H., J. E. Lee, and P. W. Carr, "The Predictive Accuracy for Estimating Infinite Dilution Activity Coefficients by γ^{∞}-Based UNIFAC," *J. Solution Chem.*, **20**, 1189 (1991).
Peres, A. M., and E. A. Macedo, "A Modified UNIFAC Model for the Calculation of Thermodynamic Properties of Aqueous and Non-aqueous Solutions Containing Sugars," *Fluid Phase Equilibr.*, **139**, 47 (1997).
Peters, C. A., K. H. Wammer, and C. D. Knightes, "Multicomponent NAPL Solidification Thermodynamics," *Transport Porous Med.*, **38**, 57 (2000).
Pividal, K. A., and S. I. Sandler, "Neighbor Effects on the Group Contribution Method-Infinite Dilution Activity-Coefficients of Binary-Systems Containing Primary Amines and Alcohols," *J. Chem. Eng. Data*, **35**, 53 (1990).
Reid, R. C., J. M. Prausnitz, and B. E. Poling, *The Properties of Gases and Liquids*, McGraw-Hill, Boston (1987).
Riley, J. P., and R. Chester, *Introduction to Marine Chemistry*, Academic Press, New York (1971).
Rogge, W. F., M. A. Mazurek, L. M. Hildemann, G. R. Cass, and B. R. T. Simoneit, "Quantification of Urban Organic Aerosols at a Molecular-Level-Identification, Abundance and Seasonal-Variation," *Atmos. Environ.*, **27A**, 1309 (1993).
Russell, L. M., and Y. Ming, "Deliquescence of Small Particles," *J. Chem. Phys.*, **116**, 311 (2002).
Russell, L. M., K. J. Noone, R. J. Ferek, R. A. Pockalny, R. C. Flagan, and J. H. Seinfeld, "Combustion Organic Aerosol as Cloud Condensation Nuclei in Ship Tracks," *J. Atmos. Sci.*, **57**, 2591 (2000).
Saxena, P., and L. M. Hildemann, "Water-Soluble Organics in Atmospheric Particles: a Critical Review of the Literature and Application of Thermodynamics to Identify Candidate Compounds," *J. Atmos. Chem.*, **24**, 57 (1996).
Saxena, P., and L. M. Hildemann, "Water Adsorption by Organics: Survey of Laboratory Evidence and Evaluation of UNIFAC for Estimating Water Activity," *Environ. Sci. Technol.*, **31**, 3318 (1997).
Saxena, P., L. M. Hildemann, P. McMurry, and J. H. Seinfeld, "Organics Alter Hygroscopic Behavior of Atmospheric Particles," *J. Geophys. Res.*, **100**, 18755 (1995).
Seinfeld, J. H., and S. N. Pandis, *Atmospheric Chemistry and Physics*, Wiley, New York (1997).
Silcock, H. L., *Solubilities of Inorganic and Organic Compounds*, Pergamon, Oxford (1979).
Skjold-Jørgensen, S., B. Kolbe, J. Gmehling, and P. Rasmussen, "Vapor-Liquid Equilibrium by UNIFAC Group Contribution. Revision and Extension," *Ind. Eng. Process Des. Dev.*, **18**, 714 (1979).
Stokes, R. H., and R. A. Robinson, "Interactions in Aqueous Nonelectrolyte Solutions: I. Solute-Solvent Equilibria," *J. Phys. Chem.*, **70**, 2126 (1966).
Sutton, C., and J. A. Calder, "Solubility of Higher-Molecular-Weight *n*-Paraffins in Distilled Water and Seawater," *Environ. Sci. Technol.*, **8**, 654 (1974).
Swietlicki, E., J. C. Zhou, D. S. Covert, K. Hämeri, B. Busch, M. Väkeva, U. Dusek, O. H. Berg, A. Wiedensohler, P. Aalto, J. Mäkelä, B. G. Martinsson, G. Papaspiropoulos, B. Mentes, G. Frank, and F. Stratmann, "Hygroscopic Properties of Aerosol Particles in the Northeastern Atlantic during ACE-2," *Tellus B* **52**, 750 (2000).
Tang, I. N., and H. R. Munkelwitz, "Water Activities, Densities, and Refractive Indices of Aqueous Sulfates and Sodium Nitrate Droplets of Atmospheric Importance," *J. Geophys. Res.*, **99**, 18801 (1994).
Tang, I. N., H. R. Munkelwitz, and N. Wang, "Water Activity Measurements with Single Suspended Droplets: The NaCl-H_2O and KCl-H_2O Systems," *J. Colloid Interface Sci.*, **114**, 409 (1986).
Turpin, B. J., J. J. Huntzicker, S. M. Larson, and G. R. Cass, "Los-Angeles Summer Midday Particulate Carbon—Primary and Secondary Aerosol," *Environ. Sci. Technol.*, **25**, 1788 (1991).
Velezmoro, C. E., and A. J. A. Meirelles, "Water Activity in Solutions Containing Organic Acids," *Dry Technol.*, **16**, 1789 (1998).
Wexler, A. S., and J. H. Seinfeld, "2nd-Generation Inorganic Aerosol Model," *Atmos. Environ. A*, **25**, 2731 (1991).
Wu, H. S., and S. I. Sandler, "Proximity Effects on the Predictions of the UNIFAC Model: 1. Ethers," *AIChE J.*, **35**, 168 (1989).
Wu, H. S., and S. I. Sandler, "Use of Ab Initio-Quantum Mechanics Calculations in Group Contribution Methods: 2. Test of New Groups in UNIFAC, " *Ind. Eng. Chem. Res.*, **30**, 889 (1991).
Yan, W. D., M. Topphoff, C. Rose, and J. Gmehling, "Prediction of Vapor-Liquid Equilibria in Mixed-Solvent Electrolyte Systems Using the Group Contribution Concept," *Fluid Phase Equilib.*, **162**, 97 (1999).
Zdenek, S., L. Strnadova, and V. Rod, "Contribution to the Application of Scaled Particle Theory to Prediction of the Salting Coefficient," *Coll. Czech. Chem. Commun.*, **45**, 679 (1980).
Zhang, S., T. Hiaki, M. Hongo, and K. Kojima, "Prediction of Infinite Dilution Activity Coeficients in Aqueous Solutions by Group Contribution Models. A Critical Evaluation," *Fluid Phase Equilib.*, **144**, 97 (1998).
Zhang, Y., C. Seigneur, J. H. Seinfeld, M. Jacobson, S. L. Clegg, and F. S. Binkowski, "A Comparative Review of Inorganic Aerosol Thermodynamic Equilibrium Modules: Similarities, Differences, and Their Likely Causes," *Atmos. Environ.*, **34**, 117 (2000).
Zhou, J., E. Swietlicki, O. H. Berg, P. P. Aalto, K. Hämeri, E. D. Nilsson, and C. Leck, "Hygroscopic Properties of Aerosol Particles over the Central Arctic Ocean during Summer," *J. Geophys. Res.*, 106, 32111 (2001).

Manuscript received Mar. 22, 2001, and revision received Nov. 27, 2001.